Bioorganic Chemistry 107 (2021) 104622

Contents lists available at ScienceDirect

Bioorganic Chemistry

journal homepage: www.elsevier.com/locate/bioorg

Isolation and characterization of neolignan derivatives with hepatoprotective and neuroprotective activities from the fruits of *Citrus medica* L. var. *Sarcodactylis* Swingle

Qin-Ge Ma [a,*], Rong-Rui Wei [a,*], Ming Yang [a], Xiao-Ying Huang [a], Fang Wang [a], Jiang-Hong Dong [b], Zhi-Pei Sang [c]

[a] Key Laboratory of Modern Preparation of Traditional Chinese Medicine of Ministry of Education & Research Center of Natural Resources of Chinese Medicinal Materials and Ethnic Medicine, Jiangxi University of Traditional Chinese Medicine, Nanchang 330004, PR China
[b] College of Chemistry and Pharmaceutical Engineering, Huanghuai University, Zhumadian 463000, PR China
[c] College of Chemistry and Pharmaceutical Engineering, Nanyang Normal University, Nanyang 473061, PR China

ARTICLE INFO

Keywords:
Citrus medica L. var. *sarcodactylis* Swingle
Neolignan
Hepatoprotective
Neuroprotective

ABSTRACT

The fruit of *Citrus medica* L. var. *sarcodactylis* Swingle is a functional food with rich nutrients and medicinal values because of its content of bioactive compounds. A bioactivity-guided chemical investigation from the fruits of *C. medica* L. var. *sarcodactylis* Swingle afforded three new benzodioxane neolignans (**1**–**3**), three new phenanthrofuran neolignan glycosides (**4**–**6**), two new biphenyl-ketone neolignans (**7**–**8**), two new 1′,7′-bilignan neolignans (**9**–**10**), as well as fourteen known neolignan derivatives (**11**–**24**), which were isolated and characterized from the fruits of *C. medica* L. var. *sarcodactylis* Swingle for the first time. These neolignan derivatives were determined by extensive and comprehensive analyzing NMR, HR-ESI-MS, UV, IR spectral data and compared with the data described in the literature. Among them, compounds **1**–**3** and **12**–**13** exhibited moderate hepatoprotective activities to improve the survival rates of HepG2 cells from 46.26 ± 1.90% (APAP, 10 mM) to 67.23 ± 4.25%, 62.87 ± 4.43%, 60.06 ± 6.34%, 56.75 ± 2.30%, 58.35 ± 6.14%, respectively. Additionally, compounds **7**–**8** and **21**–**22** displayed moderate neuroprotective activities to raise the survival rates of PC12 cells from 55.30 ± 2.25% to 66.94 ± 3.37%, 70.98 ± 5.05%, 64.64 ± 1.93%, and 62.81 ± 4.11% at 10 μM, respectively. The plausible biogenetic pathway and preliminary structure–activity relationship of the selected compounds were scientifically summarized and discussed in this paper.

1. Introduction

The fruit of *Citrus medica* L. var. *sarcodactylis* Swingle, widely well known as the bergamot or bergamot orange, belongs to the Rutaceae family [1]. It is also named as "Foshou" in Chinese because of the shape of its fruit like a finger. The fruit of *C. medica* L. var. *sarcodactylis* Swingle is used as a traditional medicinal food with the functions of relieving depressed liver, harmonizing stomach, and expelling phlegm in Chinese folk [2]. Moreover, it was used as a traditional Chinese medicine for treating hypertension, tracheitis, respiratory tract infections, angiocardiopathy, and asthma [3]. The fruits of *C. medica* L. var. *sarcodactylis* Swingle had been chemically investigated, leading to the isolation of some compounds including polysaccharides [1], flavonoids [4], cumarins [5], phenolics [6], terpenes [7], carotenoids [8], amino acids [9], and polyphenols [10]. Modern pharmacological investigations of the fruits of *C. medica* L. var. *sarcodactylis* Swingle revealed a wide variety of biological activities, including antibiofifilm [6], antibacterial [10], immunoregulatory [11], antioxidant [12], anticancer [13], antihyperglycemic [14], cardioprotective [15], and antidepressant activities [16].

Up to now, it is found that there are few reports on hepatoprotective and neuroprotective activities from the fruits of *C. medica* L. var. *sarcodactylis* Swingle. However, one article related to the neuroprotective activity of the titled species revealed that the peels of *Citrus grandis* exhibited the protection of neurons against Aβ-mediated neurotoxicity [17]. In continuation of our ongoing study more new compounds with biological activities from the fruits of *C. medica* L. var. *sarcodactylis* Swingle. A bioassay-guided investigation was carried out to find further

* Corresponding authors.
E-mail addresses: maqinge2006@163.com (Q.-G. Ma), weirongrui2011@163.com (R.-R. Wei).

https://doi.org/10.1016/j.bioorg.2020.104622
Received 11 November 2020; Received in revised form 29 December 2020; Accepted 30 December 2020
Available online 8 January 2021

hepatoprotective and neuroprotective isolates from the fruits of *C. medica* L. var. *sarcodactylis* Swingle. As a result, three new benzodioxane neolignans (**1**–**3**), three new phenanthrofuran neolignan glycosides (**4**–**6**), two new biphenyl-ketone neolignans (**7**–**8**), two new 1′,7′-bilignan neolignans (**9**–**10**), and fourteen known neolignan derivatives (**11**–**24**) (Fig. 1) were isolated from this plant for the first time. In this study, we report the isolation, characterization, bioactivity, plausible biogenetic pathway, and preliminary structure–activity

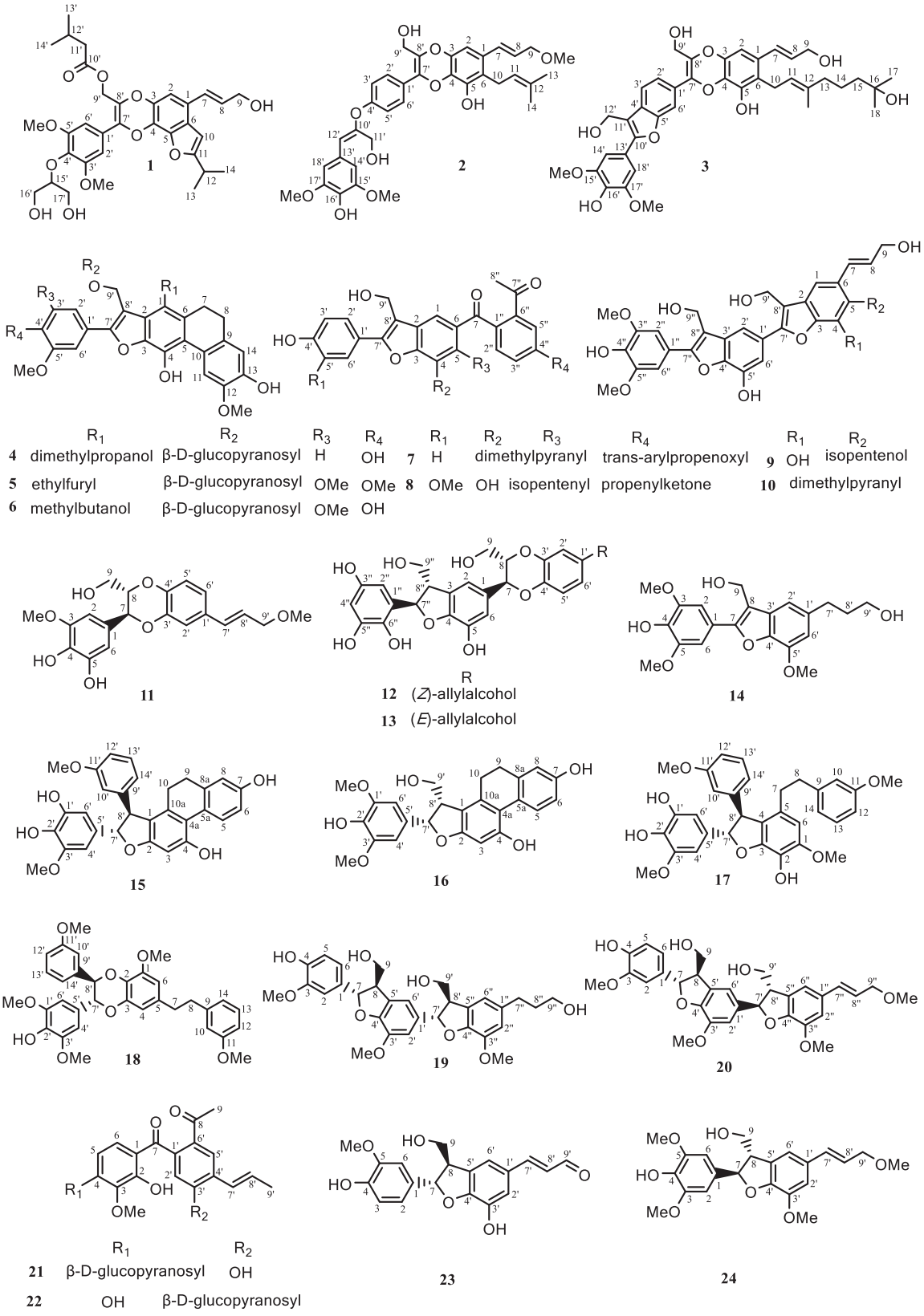

Fig. 1. Structures of compounds (**1**–**24**).

relationship of these isolates.

2. Materials and methods

2.1. General experimental procedures

A Perkin-Elmer 241 digital polarimeter at 20 ℃ was utilized to measure optical rotations. An XT5B microscopic melting point apparatus was used to measure melting points which uncorrected. An Australia GBC UV-916 spectrometer was used to measure UV spectral data. A Nicolet 5700 FT-IR spectrometer with KBr pellets was utilized to record IR spectral data. A Bruker-400 spectrometer with TMS as internal reference was applied to obtain NMR spectral data. A Q-Trap LC/MS/MS spectrometer and an Agilent 1100 series LC/MSD Trap SL mass spectrometer were utilized to measure ESI-MS and HR-ESI-MS spectral data. A CXTH LC3050N system with a YMC-pack ODS-A column (5 μm, 10 × 250 mm) was used to perform on semi-preparative HPLC. Column chromatographic separations were performed on silica gel (100–200 or 200–300 mesh), Toyopearl HW-40C, and Sephadex LH-20 columns. TLC analyses were carried out on silica gel plates (GF-254) and visualized under UV (254 nm) light and by spraying with a H_2SO_4/EtOH (1:9, v/v) solution followed by heating.

2.2. Plant material

The fruits of *C. medica* L. var. *sarcodactylis* Swingle were bought from Guangzhou, Guangdong, P. R. China, in May 2019. The plant was authenticated by Dr. Su Zhang of Wuyang Weisen Biological Medicine Co., Ltd,. The voucher specimen (No.FS-201905) deposited in Jiangxi University of TCM, Nanchang 330004, China.

2.3. Extraction and isolation

The fruits of *C. medica* L. var. *sarcodactylis* Swingle (9.5 kg) were air-dried, smashed (60 mesh), and extracted with 95% EtOH (10 L) heating under reflux at 110 °C for 4 h with electric heating jacket and round bottom flask. The same extraction procedure was performed by the above method for 3 times. The extracting solution was combined and concentrated under reduced pressure to acquire a crude extract (1.7 kg), which followed a method described previously [18–20]. The crude extract was suspended in water (2.5 L) and partitioned with solvents of petroleum ether (7.0 L), EtOAc (7.0 L), and *n*-BuOH (7.0 L), consecutively, affording petroleum ether extraction part (143.4 g), EtOAc extraction part (300.8 g), and *n*-BuOH extraction part (512.5 g), respectively. The EtOAc extraction part exhibited potential hepatoprotective [21] with improving HepG2 cell survival rate from 46.26% ± 1.90% (APAP, 10 mM) to 61.42% ± 3.41% and potential neuroprotective [22] with raising the survival rates of PC12 cells from 55.30 ± 2.25% to 67.04 ± 3.51% at 10 μM according to the biological screening results.

The EtOAc extraction part was applied to column chromatography with silica gel (100–200 mesh) and eluted by petroleum ether/EtOAc (30:1, 15:1, 8:1, 4:1, and 1:1, v/v) to afford five fractions (A_1-A_5). The A_3 (57.6 g, petroleum ether/EtOAc = 8:1, v/v) was carried out on a silica gel (200–300 mesh) column with a gradient elution (petroleum ether/EtOAc = 10:1, 8:1, and 6:1, v/v) to afford three sub-fractions (A_{3a}-A_{3c}). The A_{3b} (18.7 g, petroleum ether/EtOAc = 8:1, v/v) was performed on silica gel (200–300 mesh), Toyopearl HW-40C (95% MeOH), Sephadex LH-20 (MeOH/CH_2Cl_2 = 1:1), and semi-preparative HPLC (λ = 205–360 nm, 3 mL/min, 20–50% MeOH) columns, repeatedly, yielded **1** (7.47 mg, 30% MeOH, t_R = 31 min), **2** (8.92 mg, 35% MeOH, t_R = 39 min), **3** (9.45 mg, 33% MeOH, t_R = 35 min), **11** (12.15 mg, 35% MeOH, t_R = 45 min), **12** (14.20 mg, 32% MeOH, t_R = 36 min), **13** (13.31 mg, 35% MeOH, t_R = 45 min), **19** (11.52 mg, 35% MeOH, t_R = 39 min), **20** (15.54 mg, 32% MeOH, t_R = 37 min), **23** (8.56 mg, 30% MeOH, t_R = 42 min), and **24** (14.24 mg, 33% MeOH, t_R = 35 min). Meanwhile, the A_{3c} (21.2 g) was performed on silica gel (200–300 mesh), Sephadex LH-20 (MeOH/CH_2Cl_2 = 1:1), Toyopearl HW-40C (95% MeOH), and semi-preparative HPLC (λ = 210–380 nm, 3 mL/min, 15–45% MeOH) columns, successively, yielded **4** (7.95 mg, 25% MeOH, t_R = 28 min), **5** (9.78 mg, 30% MeOH, t_R = 37 min), **6** (8.04 mg, 28% MeOH, t_R = 34 min), **7** (11.86 mg, 30% MeOH, t_R = 35 min), **8** (8.96 mg, 32% MeOH, t_R = 44 min), **9** (12.06 mg, 30% MeOH, t_R = 34 min), **10** (9.44 mg, 33% MeOH, t_R = 46 min), **14** (12.53 mg, 32% MeOH, t_R = 40 min), **15** (12.66 mg, 34% MeOH, t_R = 51 min), **16** (7.88 mg, 30% MeOH, t_R = 47 min), **17** (13.38 mg, 33% MeOH, t_R = 45 min), **18** (16.50 mg, 32% MeOH, t_R = 41 min), **21** (9.45 mg, 26% MeOH, t_R = 31 min), and **22** (13.22 mg, 30% MeOH, t_R = 39 min).

(7*E*)-1-allyl alcohol-5,6-(11-isopropyl)-furanyl-3′,5′-dimethoxy-4′-glycerol-9′-isovalerate-3,4,7′,8′-benzodioxane neolignan (**1**): colorless powder; $[\alpha]^{20}_D$ + 4.57 (c 0.85, MeOH); mp: 204.2–204.5 °C; HR-ESI-MS: *m/z* 635.2466 $[M + Na]^+$ (calcd. for $C_{33}H_{40}O_{11}Na$, 635.2468); UV (MeOH) λ_{max} (logε): 208 (2.06), 235 (3.29), and 270 (2.57) nm; IR (KBr) ν_{max}: 3325, 2952, 1736, 1605, 1511, and 1498 cm^{-1}; ^1H NMR (DMSO-d_6, 400 MHz) and ^{13}C NMR (DMSO-d_6, 100 MHz) data see Table 1.

(7*E*,10′*E*,11*E*)-1-(9-methoxyl)-propenyl-5-hydroxy-6-prenyl-8′-methylol-11′,16′-dihydroxy-15′,17′-dimethoxy-10′-phenylallyl alcohol-3,4,7′,8′-benzodioxane neolignan (**2**): colorless powder; $[\alpha]^{20}_D$ + 3.68 (c 0.70, MeOH); mp: 206.4–206.6 °C. HR-ESI-MS: *m/z* 641.2366 $[M + Na]^+$ (calcd. for $C_{35}H_{38}O_{10}Na$, 641.2363); UV (MeOH) λ_{max} (logε): 208 (2.11), 235 (3.30), 270 (2.52), and 305 (4.17) nm; IR (KBr) ν_{max}: 3328, 1611, and 1509 cm^{-1}; ^1H NMR (DMSO-d_6, 400 MHz) and ^{13}C NMR (DMSO-d_6, 100 MHz) data see Table 1.

(7*E*,11*E*)-1-(9-methoxyl)-propenyl-5-hydroxy-6-geranyl-16′-hydroxy-15′,17′-dimethoxyphenyl-8′,11′-dimethylol-benzofuranyl-3,4,7′,8′-benzodioxane neolignan (**3**): colorless powder; $[\alpha]^{20}_D$ + 7.26 (c 0.90, MeOH); mp: 210.5–210.8 °C. HR-ESI-MS: *m/z* 725.2937 $[M + Na]^+$ (calcd. for $C_{40}H_{46}O_{11}Na$, 725.2938); UV (MeOH) λ_{max} (logε): 208 (2.09), 235 (3.34), 305 (4.09), and 343 (4.25) nm; IR (KBr) ν_{max}: 3330, 2938, 1608, and 1509 cm^{-1}; ^1H NMR (DMSO-d_6, 400 MHz) and ^{13}C NMR (DMSO-d_6, 100 MHz) data see Table 1.

1-(18,19-dimethyl)-propanol-4-hydroxyl-5,6-(13-hydroxyl-12-methoxyl)-phenylethyl-7′-(4′-hydroxyl-5′-methoxy)-phenyl-9′-O-β-D-glucopyranosyl-phenanthrofuran neolignan (**4**): colorless powder; $[\alpha]^{20}_D$ + 2.07 (c 0.45, MeOH); mp: 208.0–208.4 °C. HR-ESI-MS: *m/z* 705.2520 $[M + Na]^+$ (calcd. for $C_{36}H_{42}O_{13}Na$, 705.2523); UV (MeOH) λ_{max} (logε): 205 (2.01), 272 (3.28), 320 (3.71), and 350 (4.52) nm; IR (KBr) ν_{max}: 3421, 1610, 1518, and 1467 cm^{-1}; ^1H NMR (DMSO-d_6, 400 MHz) and ^{13}C NMR (DMSO-d_6, 100 MHz) data see Table 2.

1-(17-furanyl)-ethyl-4-hydroxyl-5,6-(13-hydroxyl-12-methoxyl)-phenylethyl-7′-(3′,4′,5′-trimethoxy)-phenyl-9′-O-β-D-glucopyranosyl-phenanthrofuran neolignan (**5**): colorless powder; $[\alpha]^{20}_D$ + 2.26 (c 0.30, MeOH); mp: 212.1–212.3 °C. HR-ESI-MS: *m/z* 757.2475 $[M + Na]^+$ (calcd. for $C_{39}H_{42}O_{14}Na$, 757.2472); UV (MeOH) λ_{max} (logε): 203 (2.04), 272 (3.22), 320 (3.27), and 346 (4.37) nm; IR (KBr) ν_{max}: 3425, 1612, and 1608 cm^{-1}; ^1H NMR (DMSO-d_6, 400 MHz) and ^{13}C NMR (DMSO-d_6, 100 MHz) data see Table 2.

1-(17*Z*)-methyl-butanol-4-hydroxyl-5,6-(13-hydroxyl-12-methoxyl)-phenylethyl-7′-(4′-hydroxy-3′,5′-dimethoxy)-phenyl-9′-O-β-D-glucopyranosyl-phenanthrofuran neolignan (**6**): colorless powder; $[\alpha]^{20}_D$ + 3.38 (c 0.58, MeOH); mp: 211.7–211.9 °C. HR-ESI-MS: *m/z* 733.2474 $[M + Na]^+$ (calcd. for $C_{37}H_{42}O_{14}Na$, 733.2472); UV (MeOH) λ_{max} (logε): 205 (2.03), 272 (3.42), 323 (3.35), and 345 (4.24) nm; IR (KBr) ν_{max}: 3423 and 1611 cm^{-1}; ^1H NMR (DMSO-d_6, 400 MHz) and ^{13}C NMR (DMSO-d_6, 100 MHz) data see Table 2.

(9′′*E*)-4,5-(11,12-dimethyl)-pyranyl-7′-(4′-hydroxy)-phenyl-4′′-propenyl-8′-methylol-furanyl-6′′-acetyl-1′′,6-biphenyl-7-ketone neolignan (**7**): colorless powder; $[\alpha]^{20}_D$ + 8.20 (c 0.85, MeOH); mp: 198.3–198.7 °C. HR-ESI-MS: *m/z* 531.1781 $[M + Na]^+$ (calcd. for $C_{32}H_{28}O_6Na$, 531.1784); UV (MeOH) λ_{max} (logε): 202 (1.89), 280 (3.61), 315 (2.43), and 330 (3.62) nm; IR (KBr) ν_{max}: 3411, 1719, 1617, and

Table 1
^{1}H NMR (400 MHz, DMSO-d_6) and ^{13}C NMR (100 MHz, DMSO-d_6) of compounds (**1**–**3**).

No.	1		2		3	
	δ_H	δ_C	δ_H	δ_C	δ_H	δ_C
1	-	124.6		131.8	-	132.0
2	6.45(s)	112.3	6.02(s)	111.4	6.04(s)	110.8
3	–	143.0	–	143.6	–	143.3
4	–	129.6	–	130.2	–	131.5
5	–	145.6	–	146.9	–	146.7
6	–	122.4	–	118.6	–	119.1
7	6.61(d,16.0)	130.4	6.52(d,16.0)	130.1	6.53(d,16.0)	130.2
8	6.29(dd,16.0,5.8)	128.9	6.21(dd,16.0,5.8)	125.9	6.20(dd,16.0,5.8)	126.1
9	4.20(d,5.8)	63.5	4.11(d,5.8)	73.1	4.13(d,5.8)	74.0
10	6.26(s)	108.6	3.48(d,7.5)	20.1	3.23(d,9.2)	21.9
11	–	161.2	5.25(t,7.5,1.5)	122.9	5.22(m)	123.9
12	3.38(m)	35.8	–	134.8	–	135.8
13	1.31(s)	23.1	1.70(s)	18.4	1.97(m)	41.1
14	1.31(s)	23.1	1.82(s)	24.3	1.46(m)	24.1
15	–	–	–	–	1.35(m)	44.2
1′	–	130.2	–	129.7	–	130.1
2′	6.58(s)	106.3	7.28(d,8.0)	127.6	7.56(dd,8.0,2.0)	121.3
3′	–	150.1	6.65(d,8.0)	118.3	7.83(d,8.0)	116.8
4′	–	131.2	–	154.2	–	126.2
5′	–	150.1	6.65(d,8.0)	118.3	–	153.0
6′	6.58(s)	106.3	7.28(d,8.0)	127.6	7.72(d,2.0)	108.8
7′	–	126.4	–	125.8	–	125.1
8′	–	125.6	–	124.3	–	124.5
9′	4.86(s)	65.3	4.18(s)	62.4	4.20(s)	62.2
10′	–	173.1	–	151.6	–	155.5
11′	2.30(d,6.6)	43.9	4.18(s)	63.8	–	115.8
12′	2.16(m)	25.1	6.21(s)	101.4	4.66(s)	55.2
13′	1.00(s)	22.1	–	124.1	–	122.1
14′	1.00(s)	22.1	6.27(s)	107.8	7.18(s)	106.2
15′	3.98(t,4.8)	84.3	–	155.0	–	149.2
16′	3.76(dd,4.8,1.0)	61.9	–	140.1	–	137.7
17′	3.76(dd,4.8,1.0)	61.9	–	155.0	–	149.2
18′	–	–	6.27(s)	107.8	7.18(s)	106.2
OCH_3-3′/5′	3.71(s)	56.5	–	–	–	–
OCH_3-15′/17′	–	–	3.86(s)	56.9	3.88(s)	57.1
OCH_3-9	–	–	3.34(s)	55.3	3.33(s)	55.0
CH_3-12	–	–	–	–	1.88(s)	16.3
CH_3-17/18	–	–	–	–	1.16(s)	29.8

1572 cm^{-1}; ^{1}H NMR (DMSO-d_6, 400 MHz) and ^{13}C NMR (DMSO-d_6, 100 MHz) data see Table 3.

(9*E*,9′′*E*)-5-isopentenyl-7′-(4′-hydroxy-5′-methoxy)-phenyl-4′′-propenylketone-8′-methylol-furanyl-6′′-acetyl-1′′,6-biphenyl-7-ketone neolignan (**8**): colorless powder; $[\alpha]^{20}_{D}$ + 7.54 (c 0.70, MeOH); mp: 200.4–200.8 °C. HR-ESI-MS: *m/z* 577.1840 $[M + Na]^+$ (calcd. for $C_{33}H_{30}H_8Na$, 577.1838); UV (MeOH) λ_{max} (logε): 202 (1.86), 280 (3.57), 318 (2.56), 332 (3.75), and 351 (4.08) nm; IR (KBr) ν_{max}: 3410, 1720, 1677, 1617, and 1573 cm^{-1}; ^{1}H NMR (DMSO-d_6, 400 MHz) and ^{13}C NMR (DMSO-d_6, 100 MHz) data see Table 3.

(7*E*,10*E*)-4,5′-dihydroxy-5-isopentenol-6-(7,8-*trans* allyl)-alcohol-7′′-(4′′-hydroxy-3′′,5′′-dimethoxyl)-phenyl-9′,9′′-dimethylol-1′,7′-bineolignan (**9**): colorless powder; $[\alpha]^{20}_{D}$ + 6.21 (c 0.64, MeOH); mp: 206.1–206.3 °C. HR-ESI-MS: *m/z* 641.1995 $[M + Na]^+$ (calcd. for $C_{34}H_{34}O_{11}Na$ 641.1999); UV (MeOH) λ_{max} (logε): 202 (1.81), 230 (2.80), and 270 (3.06) nm; IR (KBr) ν_{max}: 3409, 1611, and 1508 cm^{-1}; ^{1}H NMR (DMSO-d_6, 400 MHz) and ^{13}C NMR (DMSO-d_6, 100 MHz) data see Table 4.

(7*E*)-5′-hydroxy-4,5-(13,14-dimethyl)-pyranyl-6-allyl alcohol-7′′-(4′′-hydroxy-3′′,5′′-dimethoxyl)-phenyl-9′,9′′-dimethylol-1′,7′-bineolignan (**10**): colorless powder; $[\alpha]^{20}_{D}$ + 6.18 (c 0.51, MeOH); mp: 203.0–203.3 °C. HR-ESI-MS: *m/z* 623.1895 $[M + Na]^+$ (calcd. for $C_{34}H_{32}O_{10}Na$, 623.1893); UV (MeOH) λ_{max} (logε): 202 (1.90), 230 (2.96), 270 (3.12), and 315 (3.57) nm; IR (KBr) ν_{max}: 3410, 1612, and 1507 cm^{-1}; ^{1}H NMR (DMSO-d_6, 400 MHz) and ^{13}C NMR (DMSO-d_6, 100 MHz) data see Table 4.

2.4. Hepatoprotective activity assay

Compounds (**1**–**24**) were evaluated for hepatoprotective activities by the MTT method, which followed a method described previously [21]. HepG2 cells were fostered in 96-well plates (1×10^4 cells/well, 200 μL/well) in minimum essential media with 10% FBS and fostered for 24 h at 37 °C [23]. The compounds (**1**–**24**) and acetaminophen were added in the culture medium to give final concentrations of 10 μM and 10 mM, respectively, and incubated for 48 h at 37 °C. Additionally, the experiment selected bicyclol as the positive group and selected DMSO as the negative control group, respectively [24]. The MTT (0.5 mg/mL, 100 μL) was added to each well and incubated for 4 h at 37 °C. The absorbance of selected compounds at 570 nm was measured after adding 150 μL of DMSO. The survival rate of HepG2 cells = the mean OD of the medicated group/the mean OD of the solvent control group [25].

2.5. Neuroprotective activity assay

Compounds (**1**–**24**) were assayed for neuroprotective activities of by the MTT assay with desipramine as a positive control [22]. Compounds (**1**–**24**) were dissolved in DMSO with the final concentration of DMSO in the culture medium was 0.1% (v/v). PC12 cells were cultured in DMEM medium supplemented with 10% fetal bovine serum, 100 U/mL penicilin, and 100 μg/mL streptomycin in a humidified atmosphere of 5% CO_2 at 37 °C [22]. PC12 cells were cultured in 96-well plates (1×10^5 cells/well) [26]. The cell viability was measured by the MTT assay for a 48 h treatment. The absorbance of compounds (**1**–**24**) was recorded at 492 nm by a microplate detector. The cell viability was indicated by a

Table 2
^{1}H NMR (400 MHz, DMSO-d_6) and ^{13}C NMR (100 MHz, DMSO-d_6) of compounds (**4**–**6**).

No.	4		5		6	
	δ_H	δ_C	δ_H	δ_C	δ_H	δ_C
1	-	124.6	-	125.9	-	123.7
2	–	123.1	–	123.5	–	122.7
3	–	138.4	–	138.3	–	138.1
4	–	137.2	–	137.2	–	137.1
5	–	118.0		118.2	–	118.1
6	–	136.8	–	136.1	–	136.3
7	2.48(m)	32.6	2.47(m)	32.5	2.47(m)	32.6
8	2.42(m)	29.4	2.42(m)	29.3	2.42(m)	29.4
9	–	133.0	–	133.0	–	133.0
10	–	128.9	–	129.7	–	129.6
11	6.68(s)	115.7	6.68(s)	115.6	6.68(s)	115.6
12	–	148.6	–	148.5	–	148.5
13	–	141.5	–	141.7	–	141.6
14	6.43(s)	117.6	6.42(s)	117.8	6.42(s)	117.8
15	2.78(m)	18.1	2.25(m)	29.4	3.28(d,6.9)	31.5
16	1.58(m)	43.2	2.12(m)	24.5	6.03(m)	126.7
17	–	70.3	–	116.1	–	137.0
18	1.19(s)	29.2	7.22(s)	138.4	4.31(m)	62.9
19	1.19(s)	29.2	7.31(d,2.6)	141.3	1.74(s)	17.5
20	–	–	6.33(d,2.6)	109.4	–	–
1′	–	131.2	–	131.0	–	131.1
2′	6.98(dd,8.0,2.0)	121.4	6.39(s)	106.2	6.42(s)	104.5
3′	6.73(d,8.0)	116.8	–	149.7	–	149.4
4′	–	142.3	–	140.7	–	141.7
5′	–	149.5	–	149.7	–	149.4
6′	6.85(d,2.0)	115.4	6.39(s)	106.2	6.42(s)	104.5
7′	–	150.2	–	150.1	–	150.1
8′	–	118.9	–	119.1	–	119.0
9′	4.61(s)	53.2	4.62(s)	53.3	4.62(s)	53.3
1′’	5.01(d,7.6)	101.3	5.02(d,7.6)	101.2	5.02(d,7.6)	101.3
2′’	3.72(m)	74.2	3.71(m)	74.0	3.72(m)	74.3
3′’	3.80(m)	77.7	3.78(m)	77.6	3.79(m)	77.5
4′’	3.38(m)	71.2	3.40(m)	71.5	3.41(m)	71.4
5′’	3.68(m)	76.4	3.66(m)	76.2	3.66(m)	76.3
6′’a	3.57(dd,11.2,6.4)	63.8	3.58(dd,11.2,6.4)	64.0	3.58(dd,11.2,6.4)	64.1
6′’b	3.91(dd,11.2,3.2)	63.8	3.90(dd,11.2,3.2)	64.0	3.91(dd,11.2,3.2)	64.1
OCH_3-12	3.81(s)	57.2	3.81(s)	57.2	3.81(s)	57.2
OCH_3-5′OCH_3-4′	3.76(s)-	56.4-	3.78(s)3.78(s)	56.556.5	3.84(s)-	56.7-
OCH_3-3′	–	–	3.78(s)	56.5	3.84(s)	56.7

Table 3
^{1}H NMR (400 MHz, DMSO-d_6) and ^{13}C NMR (100 MHz, DMSO-d_6) of compounds (**7**–**8**).

No.	7 No. 7 No.		8 No.		8	
	δ_H	δ_C δ_H δ_C	δ_H	δ_C	δ_H	δ_C
1	7.25(s)	116.2 5′ 6.64(d,8.0) 118.5 1	7.23(s)	116.4 5′	-	149.3
2	–	125.7 6′ 7.39(d,8.0) 129.4 2	–	124.3 6′	6.68(d,2.0)	116.5
3	–	144.1 7′ – 152.3 3	–	144.4 7′	–	151.8
4	–	140.3 8′ – 118.3 4	–	141.3 8′	–	118.1
5	–	119.8 9′ 4.76(s) 51.6 5	–	122.2 9′	4.78(s)	52.1
6	–	132.3 1′’ – 138.3 6	–	134.6 1′’	–	138.1
7	–	189.8 2′’ 6.72(d,8.0) 123.6 7	–	189.7 2′’	6.88(dd,8.0,2.0)	124.1
8	6.64(d,10.0)	116.1 3′’ 7.43(dd,8.0,2.0) 129.4 8	3.33(d,7.5)	33.2 3′’	7.50(d,8.0)	129.2
9	5.70(d,10.0)	129.0 4′’ – 136.7 9	5.36(d,7.5)	124.4 4′’	–	136.4
10	–	79.5 5′’ 7.85(d,2.0) 125.6 10	–	132.6 5′’	7.90(d,2.0)	126.1
CH_3-11	1.47(s)	28.7 6′’ – 137.4 CH_3-11	1.80(s)	25.6 6′’	–	138.0
CH_3-12	1.47(s)	28.7 7′’ – 198.1 CH_3-12	1.68(s)	19.2 7′’	–	198.2
1′	–	131.0 CH_3-8′’ 2.55(s) 26.5 1′	–	130.8 CH_3-8′’	2.56(s)	26.5
2′	7.39(d,8.0)	129.4 9′’ 6.79(d,15.6) 125.8 2′	6.91(dd,8.0,2.0)	121.7 9′’	8.60(d,15.8)	154.7
3′	6.64(d,8.0)	118.5 10′’ 6.60(dd,15.6,6.6) 128.7 3′	6.70(d,8.0)	118.9 10′’	7.61(dd,15.8,7.8)	126.0
4′	–	158.6 CH_3-11′’ 1.95(d,6.6) 19.3 4′	–	143.1 11′’	9.60(s)	194.1

percentage of the non-treated control group [27].

3. Results and discussion

3.1. Structure elucidation of new compounds

Compound **1** was purified as a colorless powder. The HR-ESI-MS spectrum of compound **1** revealed a molecular formula $C_{33}H_{40}O_{11}$ in the light of sodium addition peak, which was determined as 635.2466 ([M + Na]$^+$ calcd. for 635.2468 for $C_{33}H_{40}O_{11}Na$), corresponding to an index of hydrogen deficiency of 14. The UV spectrum of compound **1** exhibited characteristic absorption bonds at λ_{max} 208, 235, and 270 nm, indicating the dioxane neolignan skeleton [28]. The IR spectrum of compound **1** revealed the presence of hydroxy (3325 cm^{-1}), carbonyl

Table 4
^{1}H NMR (400 MHz, DMSO-d_6) and ^{13}C NMR (100 MHz, DMSO-d_6) of compounds (**9**–**10**).

No.	9 No. 9 No.		10 No.		10	
	δ_H δ_C δ_H δ_C		δ_H δ_C		δ_H δ_C	
1	6.97(s)	112.7 4′ – 140.2 1	6.96(s)	112.6 4′	-	140.1
2	–	125.3 5′ – 142.4 2	–	125.2 5′	–	142.4
3	–	139.2 6′ 6.85(s) 110.8 3	–	139.4 6′	6.87(s)	110.9
4	–	138.0 7′ – 152.2 4	–	138.2 7′	–	152.1
5	–	116.2 8′ – 118.1 5	–	116.4 8′	–	118.0
6	–	129.6 9′ 4.68(s) 51.4 6	–	129.8 9′	4.68(s)	51.5
7	6.62(d,16.0)	130.5 1′′ – 132.7 7	6.63(d,16.0)	130.7 1′′	–	132.7
8	6.30(dt,16.0,5.8)	128.9 2′′ 6.36(s) 107.6 8	6.32(dt,16.0,5.8)	129.0 2′′	6.35(s)	107.8
9	4.21(d,5.8)	63.6 3′′ – 151.2 9	4.22(d,5.8)	63.8 3′′	–	151.4
10	6.86(d,16.7)	120.4 4′′ – 129.8 10	6.65(d,10.0)	116.3 4′′	–	129.9
11	6.78(d,16.7)	137.6 5′′ – 151.2 11	5.71(d,10.0)	129.1 5′′	–	151.4
12	–	82.6 6′′ 6.36(s) 107.6 12	–	79.5 6′′	6.35(s)	107.8
CH_3-13/14	1.50(s)	24.6 7′′ – 152.2 CH_3-13/14	1.46(s)	28.3 7′′	–	152.1
1′	–	133.1 8′′ – 118.1 1′	–	133.0 8′′	–	118.0
2′	7.21(s)	113.7 9′′ 4.68(s) 51.4 2′	7.20(s)	113.6 9′′	4.68(s)	51.5
3′	–	126.9 OCH_3-3′′/5′′ 3.79(s) 56.7 3′	–	127.0 OCH_3-3′′/5′′	3.80(s)	56.7

(1736 cm^{-1}), and benzene ring (1605, 1511, and 1498 cm^{-1}) functionalities. The ^{1}H NMR spectrum of compound **1** displayed a 7,8-*trans* allyl alcohol group [28] at δ_H 6.61 (1H, d, J = 16.0 Hz, H-7), 6.29 (1H, dt, J = 16.0, 5.8 Hz, H-8), and 4.20 (2H, d, J = 5.8 Hz, H-9) with ^{13}C NMR data δ_C 130.4 (C-7), 128.9 (C-8), and 63.5 (C-9) (Table 1), which was located at C-1 by the key HMBC correlations of H-2 to C-7 and H-8 to C-1 (Fig. 2). In the ^{1}H NMR spectrum of compound **1**, a 11-isopropyl-furan ring moiety was found at δ_H 6.26 (1H, s, H-10), 3.38 (1H, m, H-12), and 1.31 (6H, s, CH_3-13/14) with ^{13}C NMR data δ_C 108.6 (C-10), 161.2 (C-11), 35.8 (C-12), and 23.1 (C-13/14) (Table 1), which was located at C-5/6 by the key HMBC correlations of H-10 to C-5 and H-10 to C-12 (Fig. 2). Moreover, the ^{1}H NMR spectrum of compound **1** revealed a 1′,3′,4′,5′-tetrasubstituted benzene ring at δ_H 6.58 (2H, s, H-2′/6′), 3.85 (6H, s, OCH_3-3′/5′), which was attached to C-7′ by the key HMBC correlations of H-2′/6′ to C-7 (Fig. 2). A glycerol group [29] at δ_H 3.98 (1H, t, J = 4.8 Hz, H-15′) and 3.76 (4H, dd, J = 4.8, 1.0 Hz, H-16′/17′) with δ_C 84.3 (C-15′) and 61.9 (C-16′/17′) (Table 1) was connected to C-4′ by the key HMBC correlation of H-15′ to C-4′ (Fig. 2). Meanwhile, an isovalerate moiety [30] at δ_H 4.86 (1H, s, H-9′), 2.30 (2H, d, J = 6.6 Hz, H-11′), 2.16 (1H, m, H-12′), and 1.00 (6H, s, CH_3-13′/14′) with δ_C 65.3 (C-9′), 173.1 (C-10′), 43.9 (C-11′), 25.1 (C-12′), and 22.1 (C-13′/14′) (Table 1) was assigned to C-9′ by the key HMBC correlations of H_2-9′ to C-7′/10′, H-2 to C-4 (Fig. 2). The other fragments of compound **1** were connected by the key correlations of H-7 to C-9, H-2′/6′ to C-4′, H-16′ to C-17′, and H_2-9′/12′ to C-10′ in the HMBC spectrum (Fig. 2), the key correlations of H-7 to H-8, H-8 to H_2-9, H-15′ to H_2-16′, H-15′ to H_2-17′, and H_2-11′ to H-12′ in the ^{1}H–^{1}H COSY spectrum (Fig. 2), and the key correlations of H-2 to H-7, H-7 to H-9, H-6′ to H-9′, H-10 to CH_3-13, CH_3-12 to CH_3-13, CH_3-13′ to CH_3-14′, CH_3-13′ to H-11′ in the NOESY spectrum (Fig. 3). Consequently, compound **1** was determined as (7*E*)-1-allyl alcohol-5,6-(11-isopropyl)-furanyl-3′,5′-dimethoxy-4′-glycerol-9′-isovalerate-3,4,7′,8′-benzodioxane neolignan.

Compound **2** was obtained as a colorless powder. Its molecular formula was assigned as $C_{35}H_{38}O_{10}$ by HR-ESI-MS (*m/z* 641.2366 [M + Na]$^{+}$; calcd. for $C_{35}H_{38}O_{10}Na$, 641.2363), requiring 17 degrees of unsaturation. Its UV spectrum displayed absorptions at λ_{max} 208, 235, 270, and 305 nm and its IR spectrum showed absorption bonds for hydroxy (3328 cm^{-1}) and aromatic ring (1611 and 1509 cm^{-1}) groups. These characteristic absorption peaks indicated that the dioxane neolignan skeleton was in compound **2** [28]. In the ^{1}H NMR spectrum of compound **2**, a 9-methoxyl-7,8 -*trans* propenyl group [28] at δ_H 6.52 (1H, d, J = 16.0 Hz, H-7), 6.21 (1H, dd, J = 16.0, 5.8 Hz, H-8), and 4.11 (1H, d, J = 5.8 Hz, H-9) with ^{13}C NMR data δ_C 130.1 (C-7), 125.9 (C-8), and 73.1 (C-9) (Table 1) was connected to C-1 by the key HMBC correlations of H-2 to C-7 and H-8 to C-1 (Fig. 2). Moreover, a typical prenyl moiety [31] at δ_H 3.48 (2H, d, J = 7.5 Hz, H-10), 5.25 (1H, t, J = 7.5, 1.5 Hz, H-11), 1.70 (3H, s, CH_3-13), and 1.82 (3H, s, CH_3-14) (Table 1) was assigned to C-6 by the key HMBC correlation of H-11 to C-6 (Fig. 2). Meanwhile, a typical AA'BB' system [32] at δ_H 7.28 (2H, d, J = 8.0 Hz, H-2′/6′), 6.65 (2H, d, J = 8.0 Hz, H-3′/5′) (Table 1) was connected to C-7′ by the key HMBC correlations of H-2′/6′ to C-7′ (Fig. 2). Furthermore, a 11′,16′-dihydroxy-15′,17′-dimethoxy-10′-phenylallyl moiety at δ_H 4.18 (2H, s, H-11′), 6.21 (1H, s, H-12′), and 3.86 (6H, s, OCH_3-15′/17′) was connected to C-4′ by the key HMBC correlation of H-2′/6′ to C-4′ (Fig. 2). The other fragments of compound **2** was established on the key HMBC correlations of H-7 to C-9, H-10 to C-12, H-3′/5′ to C-1′, H-9′ to C-7′, H-12′ to C-11′, H-14′/18′ to C-12′/16′ (Fig. 2), the ^{1}H–^{1}H COSY correlations of H-7 to H-8, H-8 to H-9, H-10 to H-11, H-2′ to H-3′, H-5′ to H-6′ (Fig. 2), and the key NOESY correlations of H-2 to H-9, H-7 to H-9, H-9 to OCH_3-9, H-10 to CH_3-14, H-11 to CH_3-13, CH_3-13 to CH_3-14, OCH_3-15′ to H-11′, OCH_3-15′ to H-14′ (Fig. 3). Thus, compound **2** was elucidated as (7*E*,10′*E*,11*E*)-1-(9-methoxyl)-propenyl-5-hydroxy-6-prenyl-8′-methylol-11′,16′-dihydroxy-15′,17′-dimethoxy-10′-phenyl-allyl alcohol-3,4,7′,8′-benzodioxane neolignan.

Compound **3**, a colorless powder with the molecular formula of $C_{40}H_{46}O_{11}$, was demonstrated by its HR-ESI-MS at *m/z* 725.2937 [M + Na]$^{+}$ (calcd. for $C_{40}H_{46}O_{11}Na$, 725.2938) with 18 degrees of unsaturation. Its UV spectrum showed absorption bonds at λ_{max} 208, 235, 305, and 343 nm, and its IR spectrum exhibited characteristic absorption bonds at 3330, 2938, 1608, and 1509 cm^{-1}, which revealed the characteristic absorption peaks of the dioxane neolignan skeleton [28]. It was found that UV and IR spectral data of compound **3** were similar to compound **2**, which concluded compound **3** was an analogue of compound **2**. The ^{1}H and ^{13}C NMR spectral data of compound **3** were similar to compound **2**. However, there were two different replacements between compounds **3** and **2**. The H-6 was replaced by a geranyl moiety [31] at δ_H 3.23 (2H, d, J = 9.2 Hz, H-10), 5.22 (1H, m, H-11), 1.97 (2H, m, H-13), 1.46 (2H, m, H-14), 1.35 (2H, m, H-15), and 1.16 (6H, s, CH_3-17/18) (Table 1), which was verified by the key correlation of H-11 to C-6 in the HMBC spectrum (Fig. 2); and H-4′/5′ were replaced by a 16′-hydroxy-15′,17′-dimethoxyphenyl-11′-methylol-benzofuranyl group [33] at δ_H 7.18 (2H, s, H-14′/18′), 3.88 (6H, s, OCH_3-15′/17′), and 4.66 (2H, s, H-12′) (Table 1), which was determined by the key HMBC correlation of H-3′ to C-11′ (Fig. 2). Moreover, a typical ABX system at δ_H 7.56 (1H, dd, J = 8.0, 2.0 Hz, H-2′), 7.83 (1H, d, J = 8.0 Hz, H-3′), and 7.72 (1H, d, J = 2.0 Hz, H-6′) (Table 1) was assigned to C-7′ by the key HMBC correlations of H-2′/6′ to C-7′ (Fig. 2). The other fragments of compound **3** was established on the key HMBC correlations of H-7 to C-9, H-10 to C-12, H-11 to C-13, H-14 to C-12/16, H-15 to C-13, H-2′ to C-4′, H-3′ to C-1′, H-9′ to C-7′, H-12′/14′/18′ to C-10′, H-14′/18′ to C-16′ (Fig. 2), the ^{1}H–^{1}H COSY correlations of H-7 to H-8, H-8 to H-9, H-10 to H-11, H-13 to H-14, H-14 to H-15, H-2′ to H-3′ (Fig. 2), and the key

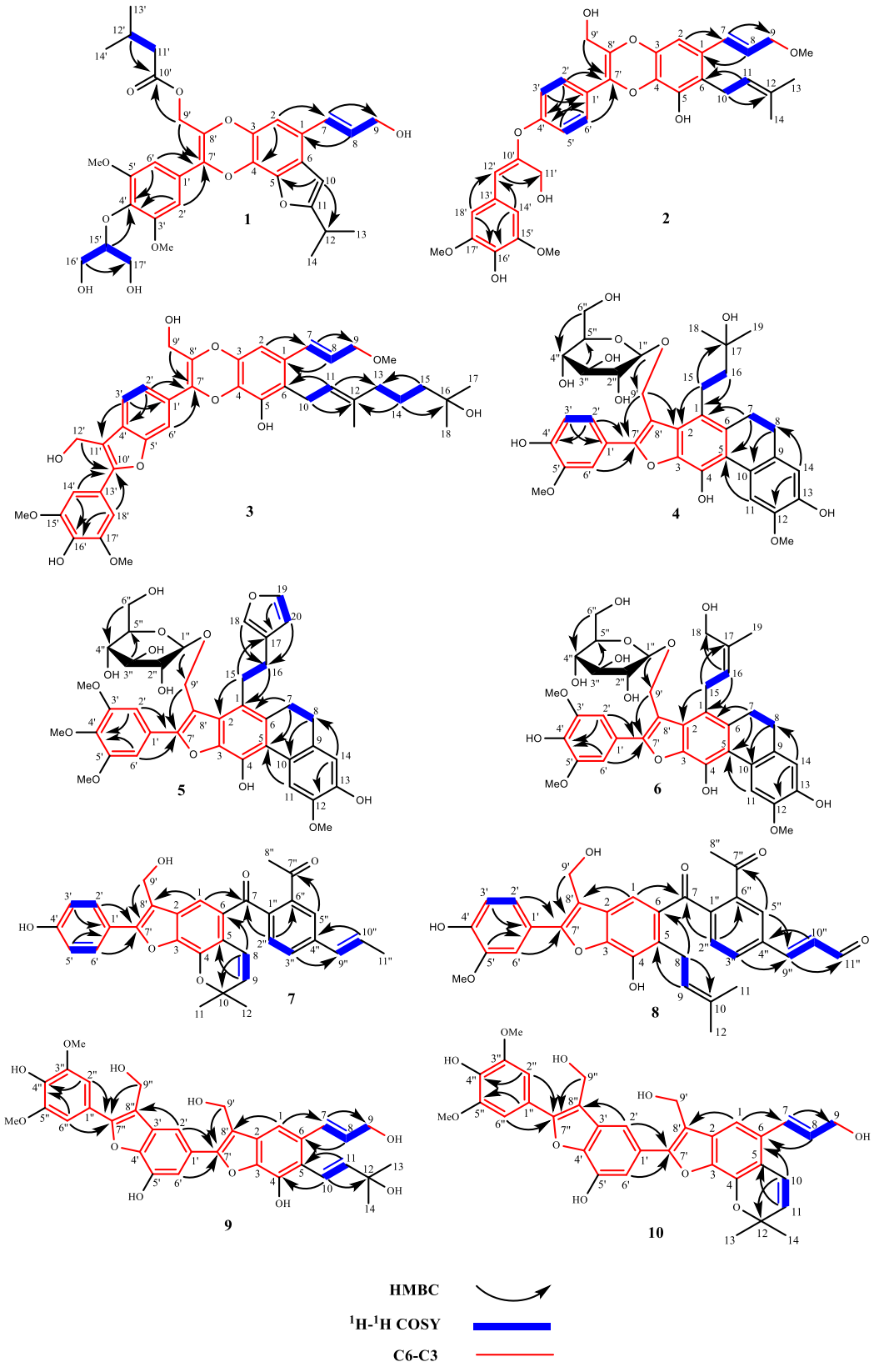

Fig. 2. Key HMBC and ^{1}H–^{1}H COSY correlations of new compounds (**1**–**10**).

NOESY correlations of H-2 to H-7, H-7 to H-9, H-9 to OCH_3-9, H-10 to CH_3-12, H-13 to H-15, H-11 to H-14, H-15 to CH_3-17, CH_3-17 to CH_3-18 (Fig. 3). Consequently, compound **3** was determined as (7*E*,11*E*)-1-(9-methoxyl)-propenyl-5-hydroxy-6-geranyl-16′-hydroxy-15′,17′-dimethoxyphenyl-8′,11′-dimethylol-benzofuranyl-3,4,7′,8′-benzodioxane neolignan.

Compound **4** was obtained as a colorless powder. It was assigned the molecular formula of $C_{36}H_{42}O_{13}$ by the HR-ESI-MS data *m/z* 705.2520

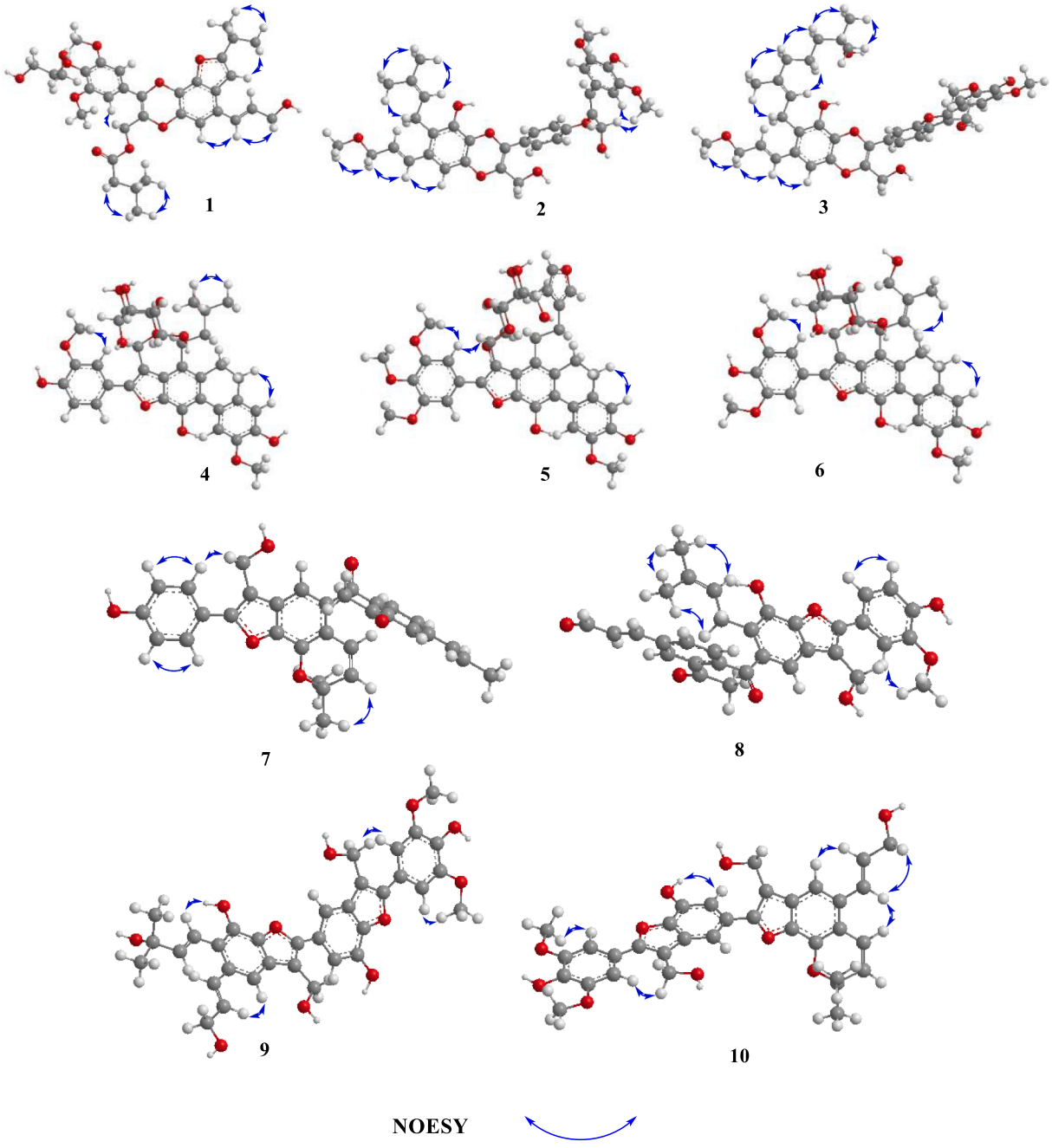

Fig. 3. Key NOESY correlations (blue) of new compounds (**1**–**10**). (For interpretation of the references to colour in this figure legend, the reader is referred to the web version of this article.)

$[M + Na]^+$ (calcd. for $C_{36}H_{42}O_{13}Na$, 705.2523), requiring 16 degrees of unsaturation. Its UV spectrum showed absorption bonds at 205, 272, 320, and 350 nm, which revealed the phenanthrofuran-type neolignan skeleton [34]. Its IR spectrum displayed absorption peaks for hydroxy (3421 cm^{-1}) and aromatic ring (1610, 1518 and 1467 cm^{-1}) functionalities. In the ^1H NMR spectrum of compound **4**, a typical 18,19-dimethylpropanol group [35] at δ_H 2.78 (2H, m, H-15), 1.58 (2H, m, H-16), and 1.19 (6H, s, CH_3-18/19) with δ_C 18.1 (C-15), 43.2 (C-16), 70.3 (C-17), and 29.2 (C-18/19) (Table 2) was assigned to C-1 by the key correlations of H_2-15 to C-2 and H_2-16 to C-1 in the HMBC spectrum (Fig. 2). Meanwhile, a typical β-glucopyranosyl moiety at δ_H 5.01 (1H, d, $J = 7.6$ Hz, H-1′′), 3.72 (1H, m, H-2′′), 3.80 (1H, m, H-3′′), 3.38 (1H, m, H-4′′), 3.68 (1H, m, H-5′′), 3.57 (1H, dd, $J = 11.2$, 6.4 Hz, H-6′′a), and 3.91 (1H, dd, $J = 11.2$, 3.2 Hz, H-6′′b) with δ_C 101.3 (C-1′′), 74.2 (C-2′′), 77.7 (C-3′′), 71.2 (C-4′′), 76.4 (C-5′′), and 63.8 (C-6′′) (Table 2) was connected to C-9′ by the key correlations of H-1′′ to C-9′, H_2-9′ to C-7′/2 in the HMBC spectrum (Fig. 2). Moreover, a typical ABX system at δ_H 6.98 (1H, dd, $J = 8.0$, 2.0 Hz, H-2′), 6.73 (1H, d, $J = 8.0$ Hz, H-3′), 6.85 (1H, d, $J = 2.0$ Hz, H-6′) (Table 2) and two methylene groups at δ_H 2.48 (2H, m, H-7), 2.42 (2H, m, H-8) were found in the ^1H NMR spectrum. The remaining fragments of compound **4** was determined by the key correlations of H_2-15 to C-17, H_2-7 to C-1/5, H_2-8 to C-10, H-11 to C-5, H-14 to C-8/12, H-2′ to C-4′/7′, H-3′ to C-1′, H-6′ to C-7′, H-3′′ to C-5′′, and H-6′′ to C-4′′ in the HMBC spectrum (Fig. 2), the key correlations of H_2-7 to H_2-8, H_2-15 to H_2-16, and H-2′ to H-3′ in the ^1H–^1H COSY spectrum (Fig. 2), and the key correlations of H-8 to H-14, H-6′ to OCH_3-5′, CH_3-18 to CH_3-19 in the NOESY spectrum (Fig. 3). Moreover, the D/L isomerism of glucose moiety was confirmed by applying HPLC analyses

after arylthiocarbamoyl-thiazolidine derivation [36]. The t_R at 17.49 min of glucose was coincided with derivatives of D-glucose, which compared with the retention times of the arythiocarbamoyl-thiazolidine [36]. Therefore, the structure of compound **4** was assigned as 1-(18,19-dimethyl)-propanol-4-hydroxyl-5,6-(13-hydroxyl-12-methoxyl)-phenylethyl-7′-(4′-hydroxyl-5′-methoxy)-phenyl-9′-O-*β*-D-glucopyranosyl-phenanthrofuran neolignan.

Compound **5** was obtained as a colorless powder, it showed an ion peak at *m/z* 757.2475 $[M + Na]^+$ in the HR-ESI-MS (calcd. for $C_{39}H_{42}O_{14}Na$, 757.2472), corresponding to the molecular formula $C_{39}H_{42}O_{14}$, indicated 19 indices of hydrogen deficiency. The UV spectrum showed characteristic absorption bonds at 203, 272, 320, 346 nm and its IR spectrum showed absorption bands for hydroxy (3425 cm^{-1}), aromatic ring (1612 and 1608 cm^{-1}) functionalities, which indicated the phenanthrofuran-type neolignan skeleton [34]. A closer comparison of the ^1H and ^{13}C NMR spectral data (Table 2) with compound **4** revealed that compound **5** was an analogue of compound **4** except for the 17-ethylfuryl group [37] at δ_H 2.25 (2H, m, H-15), 2.12 (2H, m, H-16), 7.22 (1H, s, H-18), 7.31 (1H, d, $J = 2.6$ Hz, H-19), and 6.33 (1H, d, $J = 2.6$ Hz, H-20) with δ_C 29.4 (C-15), 24.5 (C-16), 116.1 (C-17), 109.4 (C-20), 141.3 (C-19), and 138.4 (C-18) (Table 2), which was connected to C-1 by the key HMBC correlations of H_2-15 to C-2 and H_2-16 to C-1 (Fig. 2). A fragment of 3′,4′,5′-trimethoxyphenyl group at δ_H 6.39 (2H, s, H-2′/6′) and 3.78 (9H, s, OCH_3-3′/4′/5′) (Table 2) was assigned to C-7′ by the key HMBC correlations of H-2′/6′ to C-7′ (Fig. 2). The other groups of compound **5** was connected by the key HMBC correlations of H-15 to C-17, H-18/20 to C-16, H-19 to C-17, H-7 to C-1/5, H-8 to C-10, H-11 to C-5, H-14 to C-8/12, H-2′/6′ to C-4′, H-9′ to C-7′, H-3′′ to C-5′′, H-6′′ to C-4′′ (Fig. 2), the ^1H–^1H COSY correlations of H-7 to H-8, H-15 to H-16, H-19 to H-20 (Fig. 2), and the key NOESY correlations of H-8 to H-14, H-2′ to OCH_3-3′, H-2′/H-9′ (Fig. 3). Moreover, the D/L isomerism of glucose moiety was confirmed by applying HPLC analyses after arylthiocarbamoyl-thiazolidine derivation [36]. The t_R at 17.48 min of glucose was coincided with derivatives of D-glucose, which compared with the retention times of the arythiocarbamoyl-thiazolidine [36]. Consequently, compound **5** was elucidated as 1-(17-furanyl)-ethyl-4-hydroxyl-5,6-(13-hydroxyl-12-methoxyl)-phenylethyl-7′-(3′,4′,5′-trimethoxy)-phenyl-9′-O-*β*-D-glucopyranosyl-phenanthrofuran neolignan.

Compound **6** was isolated as a colorless powder. The molecular formula of compound **6** was deduced as $C_{37}H_{42}O_{14}$ in view of its HR-ESI-MS (*m/z* 733.2474, $[M + Na]^+$; calcd. for 733.2472), indicating 17 indices of hydrogen deficiency. The UV spectrum of compound **6** exhibited the characteristic absorption bonds of the phenanthrofuran-type neolignan skeleton at 205, 272, 323, and 345 nm [34]. Its IR spectrum exhibited the characteristic adsorptions at 3423 and 1611 cm^{-1} suggesting hydroxy group and benzene ring group, respectively. The ^1H and ^{13}C NMR spectral data indicated that the chemical structure of compound **6** resembled that of compound **5**, except that the (17*Z*)-methyl-butanol group [38] at δ_H 3.28 (2H, d, $J = 6.9$ Hz, H-15), 6.03 (1H, m, H-16), 4.31 (2H, m, H-18), and 1.74 (3H, s, CH_3-19) with δ_C 31.5 (C-15), 126.7 (C-16), 137.0 (C-17), 62.9 (C-18), and 17.5 (C-19) (Table 2) was located to C-1 by the key HMBC correlations of H_2-15 to C-2 and H_2-16 to C-1 (Fig. 2), and a 4′-hydroxy-3′,5′-dimethoxyphenyl group at δ_H 6.42 (2H, s, H-2′/6′) and 3.84 (6H, s, OCH_3-3′/5′) (Table 2) was assigned to C-7′ by the key HMBC correlations of H-2′/6′ to C-7′ (Fig. 2). The other groups of compound **6** was connected by the key HMBC correlations of H-15 to C-17, H-16 to C-18, H-7 to C-1/5, H-8 to C-10, H-11 to C-5, H-14 to C-8/12, H-2′/6′ to C-4′, H-9′ to C-7′, H-3′′ to C-5′′, H-6′′ to C-4′′ (Fig. 2), the ^1H–^1H COSY correlations of H-7 to H-8, H-15 to H-16 (Fig. 2), and the key NOESY correlations of H-8 to H-14, H-2′ to OCH_3-3′, H-16/CH_3-19 (Fig. 3). Moreover, the D/L isomerism of glucose moiety was confirmed by applying HPLC analyses after arylthiocarbamoyl-thiazolidine derivation [36]. The t_R at 17.50 min of glucose was coincided with derivatives of D-glucose, which compared with the retention times of the arythiocarbamoyl-thiazolidine [36]. Therefore, compound **6** was determined as 1-(17*Z*)-methyl-butanol-4-hydroxyl-5,6-(13-hydroxyl-12-methoxyl)-phenylethyl-7′-(4′-hydroxy-3′,5′-dimethoxy)-phenyl-9′-O-*β*-D-glucopyranosyl-phenanthrofuran neolignan.

Compound **7** was isolated as a colorless powder, and its molecular formula was established as $C_{32}H_{28}O_6$ through HR-ESI-MS (*m/z* 531.1781, $[M + Na]^+$; calcd. for 531.1784) and NMR spectroscopic data, suggesting 19 indices of hydrogen deficiency. Its UV spectrum showed the absorption bonds at λ_{max} 202, 280, 315, and 330 nm and IR spectrum showed characteristic absorption bonds at hydroxy (3411 cm^{-1}), carbonyl (1719 cm^{-1}), and aromatic ring (1617 and 1572 cm^{-1}) functional groups, which revealed compound **7** contained the biphenyl ketone-type neolignan skeleton [39]. The ^1H and ^{13}C NMR spectra showed the 11,12-dimethylpyranyl moiety [40] at δ_H 6.64 (1H, d, $J = 10.0$ Hz, H-8), 5.70 (1H, d, $J = 10.0$ Hz, H-9), and 1.47 (6H, s, CH_3-11/12) with δ_C 116.1 (C-8), 129.0 (C-9), 79.5 (C-10), and 28.7 (C-11/12) (Table 3) was assigned to C-4/5 by the key HMBC correlations of H-9 to C-5 and H-8 to C-6 (Fig. 2). Additionally, analysis of its NMR data indicated the presence of a 9′′,10′′-*trans* propenyl unit [39] at δ_H 6.79 (1H, d, $J = 15.6$ Hz, H-9′′), 6.60 (1H, dd, $J = 15.6$, 6.6 Hz, H-10′′), and 1.95 (3H, d, $J = 6.6$ Hz, CH_3-11′′) with δ_C 125.8 (C-9′′), 128.7 (C-10′′), and 19.3 (C-11′′) (Table 3) was connected to C-4′′ by the key HMBC correlations of H-3′′ to C-9′′ and H-10′′ to C-4′′ (Fig. 2). Meanwhile, an acetyl group at δ_H 2.55 (3H, s, CH_3-8′′) was attached to C-6′′ by the HMBC correlation of H-5′′ to C-7′′ (Fig. 2) and a 4′-hydroxy phenyl group at δ_H 7.39 (2H, d, $J = 8.0$ Hz, H-2′/6′) and 6.64 (2H, d, $J = 8.0$ Hz, H-3′/5′) (Table 3) was assigned to C-7′ by the HMBC correlations of H-2′/6′ to C-7′ (Fig. 2). The remaining groups of compound **7** was elucidated by the key HMBC correlations of H-1 to C-7/8′, H-8 to C-6/10, H-9 to C-5, H-3′/5′ to C-1′, H-9′ to C-7′, H-2′′ to C-7/6′′, and H-5′′ to C-7′′ (Fig. 2), the key ^1H–^1H COSY correlations of H-8 to H-9, H-2′ to H-3′, H-5′ to H-6′, H-2′′ to H-3′′, and H-9′′ to H-10′′ (Fig. 2), and the key correlations of H-2′/H-9′, H-2′/H-3′, H-5′/H-6′, CH_3-12/H-9 in the NOESY spectrum (Fig. 3). Consequently, compound **7** was elucidated as (9′′*E*)-4,5-(11,12-dimethyl)-pyranyl-7′-(4′-hydroxy)-phenyl-4′′-propenyl-8′-methylol-furanyl-6′′-acetyl-1′′,6-biphenyl-7-ketone neolignan.

Compound **8** was isolated as a colorless powder. Its molecular formula was determined to be $C_{33}H_{30}H_8$, based on HR-ESI-MS data at *m/z* 577.1840 $[M + Na]^+$ (calcd. for $C_{33}H_{30}H_8Na$, 577.1838), corresponding to 19 degrees of unsaturation. It was concluded that compound **8** was an analogue of compound **7** with the biphenyl ketone-type neolignan skeleton [39] by comparing with the UV (λ_{max} 202, 280, 318, 332, and 351 nm) and IR (3410, 1720, 1677, 1617, and 1573 cm^{-1}). Detailed analysis of the ^1H and ^{13}C NMR spectral data (Table 3) revealed that compound **8** was similar to those of compound **7** except for an isopentenyl [21] group at δ_H 3.33 (2H, d, $J = 7.5$ Hz, H-8), 5.36 (1H, d, $J = 7.5$ Hz, H-9), 1.80 (3H, s, CH_3-11), and 1.68 (3H, s, CH_3-12) (Table 3), and above moiety was connected to C-5 by the key HMBC correlations of H-9 to C-5 and H_2-8 to C-6 (Fig. 2). Meanwhile, a group of characteristic peaks of a propenylketone group [41] at δ_H 8.60 (1H, d, $J = 15.8$ Hz, H-9′′), 7.61 (1H, dd, $J = 15.8$, 7.8 Hz, H-10′′), and 9.60 (1H, brs, H-11′′) with δ_C 154.7 (C-9′′), 126.0 (C-10′′), and 194.1 (C-11′′) (Table 3) was assigned to C-4′′ by the key HMBC correlations of H-3′′/5′′ to C-9′′ and H-10′′ to C-4′′ (Fig. 2). Moreover, two typical ABX systems at δ_H 6.91 (1H, dd, $J = 8.0$, 2.0 Hz, H-2′), 6.70 (1H, dd, $J = 8.0$ Hz, H-3′), 6.86 (1H, d, $J = 2.0$ Hz, H-5′) and 6.88 (1H, dd, $J = 8.0$, 2.0 Hz, H-2′′), 7.50 (1H, d, $J = 8.0$ Hz, H-3′′), 7.90 (1H, d, $J = 2.0$ Hz, H-5′′) were found in the ^1H NMR spectrum of compound **8**. The other groups of compound **8** was determined by the key HMBC correlations of H-1 to C-7/8′, H-8 to C-6/10, H-9 to C-5, H-3′/5′ to C-1′, H-9′ to C-7′, H-2′′ to C-6′′/7, H-3′′ to C-9′′, H-5′′ to C-7′′/9′′, H-9′′ to C-11′′, H-10′′ to C-4′′ (Fig. 2), the ^1H–^1H COSY correlations of H-8 to H-9, H-2′ to H-3′, H- 2′′ to 3′′, H-9′′ to H-10′′, H-10′′ to H-11′′ (Fig. 2), and the key NOESY correlations of H-8 to CH_3-11, H-9 to CH_3-12, CH_3-11 to CH_3-12, H-2′ to H-3′, H-6′ to OCH_3-5′ (Fig. 3). Thus, compound **8** was elucidated as (9*E*,9′′*E*)-5-isopentenyl-7′-(4′-hydroxy-5′-methoxy)-phenyl-4′′-propenylketone-8′-methylol-furanyl-6′′-acetyl-1′′,6-biphenyl-7-ketone neolignan.

Compound **9** was isolated as a colorless powder. Its molecular formula was confirmed as $C_{34}H_{34}O_{11}$ based on the HR-ESI-MS data (*m/z* 641.1995 $[M + Na]^+$, calcd. for $C_{34}H_{34}O_{11}Na$ 641.1999), indicating 18 indices of hydrogen deficiency. Its UV spectrum showed absorption bonds at 202, 230, and 270 nm, along with IR absorption of hydroxy (3409 cm^{-1}) and aromatic ring (1611 and 1508 cm^{-1}) functional groups, which concluded the 1′,7′-bineolignan skeleton [42]. In the ^1H NMR spectrum of compound **9**, an isopentenol moiety at δ_H 6.86 (1H, d, $J = 16.7$ Hz, H-10), 6.78, 1H, d, $J = 16.7$ Hz, H-11), and 1.50 (6H, s, CH_3-13/14) with δ_C 120.4 (C-10), 137.6 (C-11), 82.6 (C-12), and 24.6 (C-13/14) (Table 4) was assigned to C-5 by the key HMBC correlations of H-11 to C-5 and H-10 to C-4 (Fig. 2). In addition, a 7,8-*trans* allyl alcohol group [28] at δ_H 6.62 (1H, d, $J = 16.0$ Hz, H-7), 6.30 (1H, dt, $J = 16.0$, 5.8 Hz, H-8), and 4.21 (2H, d, $J = 5.8$ Hz, H-9) and ^{13}C NMR data δ_C 130.5 (C-7), 128.9 (C-8), and 63.6 (C-9) (Table 4) was assigned to C-6 by the key HMBC correlations of H-1 to C-7 and H-8 to C-6 (Fig. 2). Moreover, a moiety of 4′′-hydroxy-3′′,5′′-dimethoxyl phenyl at δ_H 6.36 (2H, s, H-2′′/6′′) and 3.79 (6H, s, OCH_3-3′′/5′′) (Table 4) was connected to C-7′′ by the key correlations of H-2′′/6′′ to C-7′′ in the HMBC spectrum (Fig. 2). The structure of compound **9** was further confirmed by analyses of the key HMBC correlations of H-1 to C-8′, H-7 to C-9, H-10 to C-12, H-2′ to C-7′/8′′, H-6′ to C-7′, H_2-9′ to C-7′, H-2′′/6′′ to C-4′′, and H_2-9′′ to C-7′′ (Fig. 2), the key ^1H–^1H COSY correlation of H-7 to H-8, H-8 to H_2-9, and H-10 to H-11 (Fig. 2), and the key correlations of H-1 to H-8, 4-OH to H-10, H-2′′ to H-9′′, H-6′′ to 5′′–OCH_3 in the NOESY spectrum (Fig. 3). Therefore, compound **9** was determined as (7*E*,10*E*)-4,5′-dihydroxy-5-isopentenol-6-(7,8-*trans* allyl)-alcohol-7′′-(4′′-hydroxy-3′′,5′′-dimethoxyl)-phenyl-9′,9′′-dimethylol-1′,7′-bineolignan.

Compound **10** was obtained as a colorless powder. Its molecular formula was established as $C_{34}H_{32}O_{10}$ by HR-ESI-MS (*m/z* 623.1895 $[M + Na]^+$, calcd. for $C_{34}H_{32}O_{10}Na$, 623.1893), corresponding to 19 degrees of unsaturation. Its UV spectrum exhibited absorptions at λ_{max} 202, 230, 270, and 315 nm and IR spectrum showed hydroxy (3410 cm^{-1}) and aromatic ring (1612 and 1507 cm^{-1}) functional groups, it was concluded that compound **10** was an analogue of compound **9**. A closer comparison of the NMR spectra (Table 4) with compound **9** revealed that compound **10** contained the 1′,7′-bineolignan skeleton [42]. The only difference between compounds **10** and **9** was the appearance of the 13,14-dimethyl-pyran moiety [40] at δ_H 6.65 (1H, d, $J = 10.0$ Hz, H-10), 5.71 (1H, d, $J = 10.0$ Hz, H-11), and 1.46 (6H, s, CH_3-13/14) with δ_C 116.3 (C-10), 129.1 (C-11), 79.5 (C-12), and 28.3 (C-13/14) (Table 4), which was assigned to C-4/5 by the key HMBC correlations of H-11 to C-5 and H-10 to C-6 (Fig. 2). The other fragments of compound **10** were connected by the key HMBC correlations of H-1 to C-7/8′′, H-7 to C-9, H-8 to C-6,H-10 to C-12, H-14 to C-12, H-2′/6′ to C-7′, H-2′ to C-8′, H-9′ to C-7′, H-2′′/6′′ to C-4′′/7′′, H-9′′ to C-7′′ (Fig. 2), the ^1H–^1H COSY correlation of H-7 to H-8, H-8 to H-9, H-10 to H-11 (Fig. 2), and the key NOESY correlations of H-1 to H-8, H-7 to H-9, H-7 to H-10, 5′-OH to H-6′, H-2′′ to H-9′′, H-6′′ to OCH_3-5′′ (Fig. 3). Thus, compound **10** was determined as (7*E*)-5′-hydroxy-4,5-(13,14-dimethyl)-pyranyl-6-allyl alcohol-7′′-(4′′-hydroxy-3′′,5′′-dimethoxyl)-phenyl-9′,9′′-dimethylol-1′,7′-bineolignan.

Meanwhile, fourteen known neolignan derivatives (**11**–**24**) were isolated and characterized from the fruits of *C. medica* L. var. *sarcodactylis* Swingle for the first time. These isolates were elucidated to be (7*S*,8*R*)-9′,3-dimethoxyl isoamericanol a (**11**) [28], (7*S*,8*R*,7′′*S*,8′′*R*)-7,8–7′′,8′′-*trans*-7′,8′-*Z*-sesquiverniciasin A (**12**) [28], (7*S*,8*R*,7′′*S*, 8′′*R*)-7,8–7′′,8′′-*trans*-7′,8′-*E*-sesquiverniciasin A (**13**) [27], selamoellenin B (**14**) [33], dendronbibisline A (**15**) [34], dendronbibisline B (**16**) [34], dendronbibisline C (**17**) [34], dendronbibisline D (**18**) [34], herpetosiols B (**19**) [42], herpetosiols C (**20**) [42], silychristin A (**21**) [39], silychristin B (**22**) [39], (7*S*,8*R*)-*threo*-1′-[3′-hydroxy-7-(4-hydroxy-3-methoxyphenyl)-8-hydroxymethyl-7,8-dihydrobenzofuran]acryl-aldehyde (**23**) [41], and (-)-(7*R*,8*S*,7′*E*)-4-hydroxy-3,5,5′,9′-tetramethoxy-4′,7-epoxy-8,3′-neolign-7′-en-9-ol (**24**) [43] by comparison of their spectroscopic data and references.

3.2. Acid hydrolysis of compounds 4–6 and 21–22

Compounds **4**–**6** and **21**–**22** (5 mg each) were treated in 5% HCl (0.5 mL) and heated at 90 °C for 2 h, respectively [44]. After cooling, each reaction mixture was extracted with EtOAc, and the aqueous layer was neutralised with 0.1 M NaOH. As a result, the glucoses were obtained from compounds **4**–**6** and **21**–**22**, which were detected by thin layer chromatography (TLC) with authentic sugars. The type of glucose was identified by TLC method with authentic sugar [45]. Meanwhile, we had confirmed the D/L isomerism of glucose moiety by applying reversed-phase HPLC analyses after arylthiocarbamoyl-thiazolidine derivation [36]. The glucoses were obtained from compounds **4**–**6** and **21**–**22**, and they were dried *in vacuo*. The residue was dissolved in pyridine (0.1 mL) containing L-cysteine methyl ester hydrochloride (0.5 mg) and heated at 60 °C for 1 h. A 0.1 mL solution of O-torylisothiocyanate (0.5 mg) in pyridine was added to the mixture, which was heated at 60 °C for 1 h. The reaction mixture was directly analyzed by reversed-phase HPLC. The t_R values of peaks in the range of 17.48–17.50 min were coincided with derivatives of D-glucose, which compared with the retention times of the arythiocarbamoyl-thiazolidine [36].

3.3. Plausible biogenetic pathways of compounds (1–10)

It's very important that the structures of compounds (**1**–**10**) were determined as neolignan derivatives, which may be closely related to biogenetic pathways, were isolated from *C. medica* L. var. *sarcodactylis* Swingle at the same time (Scheme 1). Interestingly, the plausible biogenetic pathway of compounds (**1**–**3**) could be traced back to benzodioxane neolignan core just like many neolignans. Compound **1** went through hydrolysis of ester bond to obtain compound **2**, and compound **2** went through cyclization to afford compound **1**. Compound **2** went through cyclization and substitution to obtain compound **3**. Meanwhile, the plausible biogenetic pathway for compounds (**4**–**6**) could be traced back to phenanthrofuran neolignan skeleton, which mainly went through a series of potential substitution to obtain compounds (**4**–**6**). Thus, compounds **4** and **6** went through cyclization to obtain compound **5**, and compound **5** went through substitution to obtain compounds **4** and **6**. In the same way, the plausible biogenetic pathway of compound **7** could be readily transformed to compound **8** went through the way of ring opening and compound **8** transformed to compound **7** went through cyclization. Moreover, the plausible biogenetic pathway of compound **9** could be readily changed to compound **10** by the way of cyclization and compound **10** transformed to compound **9** went through the way of ring opening. The further and reasonable biogenetic pathway of compounds (**1**–**10**) of *C. medica* L. var. *sarcodactylis* Swingle will be researched in the future.

3.4. Statistical analysis of hepatoprotective and neuroprotective activities

In this study, compounds (**1**–**24**) were evaluated for their hepatoprotective activities in HepG2 cells by the acetaminophen (APAP)-induced damage model at 10.0 μM with bicyclol as a positive group (cell viability of 75.34 ± 3.60%). As a result, compounds **1**–**3** and **12**–**13** exhibited moderate hepatoprotective activities to improve the HepG2 cell survival rates from 46.26 ± 1.90% (APAP, 10 mM) to 67.23 ± 4.25%, 62.87 ± 4.43%, 60.06 ± 6.34%, 56.75 ± 2.30%, and 58.35 ± 6.14%, respectively (Fig. 4). Among them, compounds (**1**–**3**) showed slightly better cell viabilities than compounds (**12**–**13**). However, the other compounds displayed no hepatoprotective activities. Meanwhile, compounds (**1**–**24**) were also assayed for their neuroprotective activities on PC12 cells with desipramine as a positive control (cell viability of 79.84 ± 1.55%). As shown in Fig. 5, compounds **7**, **8**, **21**, and **22** showed certain neuroprotective activities to raise the survival rates of PC12 cells from 55.30 ± 2.25% to 66.94 ± 3.37%, 70.98 ± 5.05%, 64.64 ± 1.93%, and 62.81 ± 4.11% at 10 μM, respectively. Among them, compounds **7** and **8** showed slightly better neuroprotective activities with cell

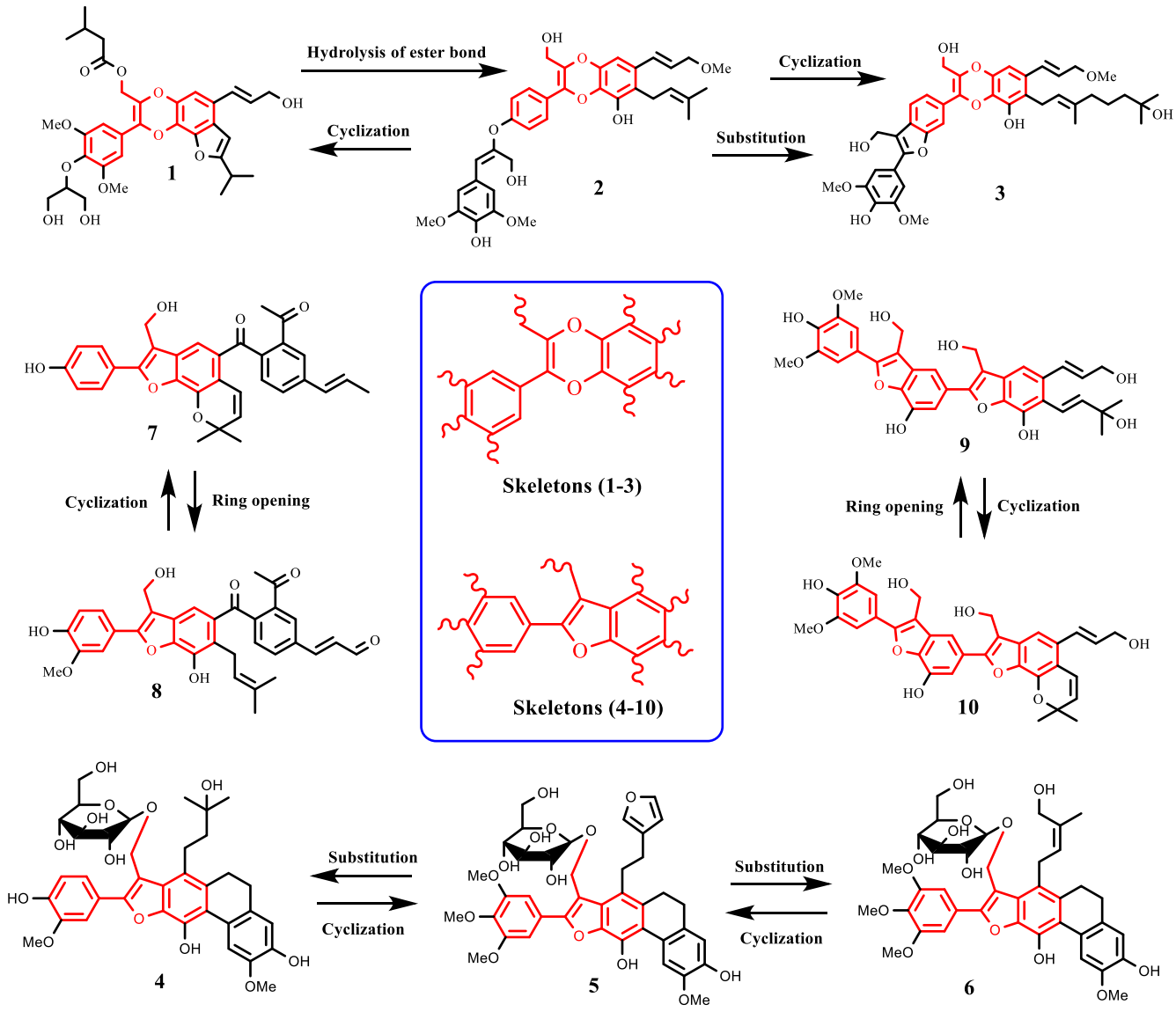

Scheme 1. Plausible biogenetic pathways of new compounds (**1**–**10**).

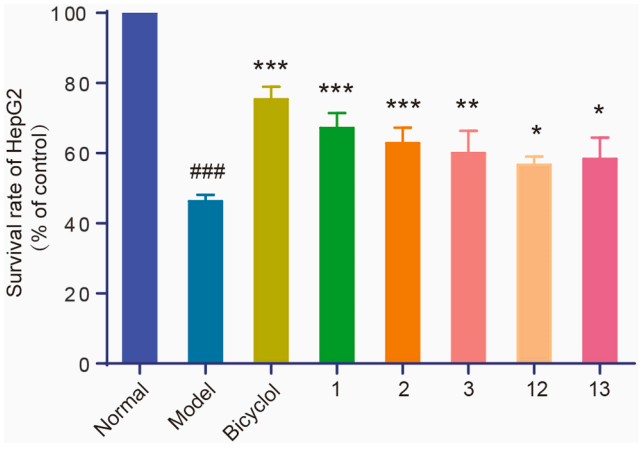

Fig. 4. Hepatoprotective activities of selected compounds (10 μM). $n = 3$, mean ± SD. $^{###}P < 0.001$, compared with normal; $^{*}P < 0.05$, $^{***}P < 0.001$, compared with model.

viabilities of 66.94 ± 3.37% and 70.98 ± 5.05% than compounds **21** and **22** with cell viabilities of 64.64 ± 1.93% and 62.81 ± 4.11% at 10 μM. However, the other compounds exhibited no neuroprotective activities in this experiment. This study will enrich the chemical constituents of *C. medica* L. var. *sarcodactylis* Swingle and facilitate the development of more hepatoprotective and neuroprotective agents in the future.

3.5. Preliminary structure activity relationship of active compounds

A preliminary structure–activity relationship of neolignan derivatives (**1**–**24**) was summarized according to their chemical structures and hepatoprotective and neuroprotective activities. Compounds **1**–**3** and **12**–**13** displayed certain hepatoprotective activities which possessed the same benzodioxane skeleton. Among them, compounds (**1**–**3**) exhibited the most obvious cell survival rates of 67.23 ± 4.25%, 62.87 ± 4.43%, and 60.06 ± 6.34%, respectively, which had the same substitutions of 5-hydroxy-6-prenyl moiety which possibly dominated their hepatoprotective activities. Meanwhile, compounds **7**–**8** and **21**–**22** exhibited certain neuroprotective activities which possessed the same biphenyl-ketone skeleton. Among them, compounds (**7**–**8**) showed the most important neuroprotective activities with increasing the cell survival rate at 66.94 ± 3.37% and 70.98 ± 5.05% at 10 μM,

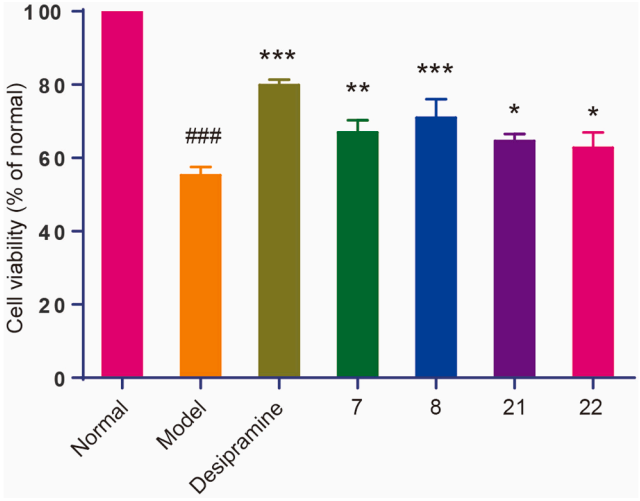

Fig. 5. Neuroprotective activities of selected compounds against corticosterone-induced neuronal injury in PC12 cells (10 μM). $n = 3$, mean ± SD. $^{###}P < 0.001$, compared with normal; $^{*}P < 0.05$, $^{**}P < 0.01$, $^{***}P < 0.001$, compared with model.

respectively. It is the reason that C-2/3 was replaced by the benzofuran moiety, which possibly played an important role in mediating neuroprotective activities. The structure–activity relationship of hepatoprotective and neuroprotective compounds from *C. medica* L. var. *sarcodactylis* Swingle need further research in the future.

4. Conclusion

In this work, three new benzodioxane neolignans (**1**–**3**), three new phenanthrofuran neolignan glycosides (**4**–**6**), two new biphenyl-ketone neolignans (**7**–**8**), two new 1′,7′-bilignan neolignans (**9**–**10**), along with fourteen known neolignan derivatives (**11**–**24**) were isolated from the fruits of *C. medica* L. var. *sarcodactylis* Swingle for the first time. Among them, compounds **1**–**3** and **12**–**13** exhibited moderate hepatoprotective activities to improve the survival rates of HepG2 cells from 46.26 ± 1.90% (APAP, 10 mM) to 67.23 ± 4.25%, 62.87 ± 4.43%, 60.06 ± 6.34%, 56.75 ± 2.30%, 58.35 ± 6.14%, respectively. Compounds (**1**–**3**) showed slightly better cell viabilities than compounds (**12**–**13**). Additionally, compounds **7**–**8** and **21**–**22** displayed moderate neuroprotective activities to raise the survival rates of PC12 cells from 55.30 ± 2.25% to 66.94 ± 3.37%, 70.98 ± 5.05%, 64.64 ± 1.93%, and 62.81 ± 4.11% at 10 μM, respectively. Compounds **7** and **8** showed slightly better neuroprotective activities than compounds **21** and **22**. These findings shed much light on a better understanding of the hepatoprotective and neuroprotective activities of these neolignan derivatives and provided new insights into developing better hepatoprotective and neuroprotective drugs in the future.

Declaration of Competing Interest

The authors declare that they have no known competing financial interests or personal relationships that could have appeared to influence the work reported in this paper.

Acknowledgements

This work was supported by Jiangxi Provincial Natural Science Foundation (20202BAB206078, 20202BAB216036), the Scientific Research Project of Jiangxi Administration of Traditional Chinese Medicine (2019A002, 2019A018), the Key Scientific Research Project of Colleges and Universities in Henan Province (19A350006), the National Natural Science Foundation of China (81803843), the Science and Technology Project of Jiangxi Health Commission (20195648, 20195650), the Science and Technology Project of Jiangxi Provincial Department of Education (GJJ180662, GJJ180688), the Doctoral Research Initiation Fund Project of Jiangxi University of TCM (2018BSZR007, 2018BSZR010), and the Scientific Research Project of First-class Discipline of Chinese Materia Medica of Jiangxi University of TCM (JXSYLXK-ZHYAO027, JXSYLXK-ZHYAO032) .

References

[1] Y. Gao, B. Peng, Y.F. Xu, J.N. Yang, L.Y. Song, S.X. Bi, Y.Y. Chen, J.H. Zhu, Y. Wen, R.M. Yu, Structural characterization and immunoregulatory activity of a new polysaccharide from *Citrus* medica L. var *Sarcodactylis*, RSC Adv. 9 (2019) 6603–6612.
[2] S.D. Zhang, H.Y. Yang, J. Zeng, M. Li, Research progress of *Citrus* medica L. var *Sarcodactylis*, China J. Trad. Chin. Med. Pharm. 33 (2018) 3510–3514.
[3] Z.C. He, F.G. Liang, Y.Y. Zhang, Y.J. Pan, Water-soluble polysaccharides from finger citron fruits (*Citrus medica* L. var. *sarcodactylis*), Carbohydr. Res. 388 (2014) 100–104.
[4] X. Deng, X.M. Huang, D. Wu, Process optimization of total flavonoids from chuan bergamot by supercritical CO_2 extraction, J. Chongqing Univ. Arts Sci. 33 (2014) 94–98.
[5] G.L. Cui, L.Y. Li, J. Tan, Y. Zhang, Analysis and evaluation of eight active ingredients in *Citrus medica* L. var. *sarcodactylis* Swingle from different regions, Nat. Prod. Res. Dev. 31 (2019) 250–260.
[6] E.W. Wang, Y.Q. Li, B.L. Maguy, Z.X. Lou, H.X. Wang, W.Q. Zhao, X.H. Chen, Separation and enrichment of phenolics improved the antibiofifilm and antibacterial activity of the fractions from *Citrus medica* L. var. *sarcodactylis* in vitro and in tofu, Food Chem. 294 (2019) 533–538.
[7] A. Verzera, A. Trozzi, M. Zappalá, C. Condurso, A. Cotroneo, Essential oil composition of *Citrus meyerii* Y. Tan. and *Citrus medica* L. cv. Diamante and their lemon hybrids, J. Agric. Food Chem. 53 (2005) 4890–4894.
[8] A.L. Fanciullino, C. Dhuique-Mayer, F. Luro, J. Casanova, R. Morillon, P. Ollitrault, Carotenoid diversity in cultivated citrus is highly influenced by genetic factors, J. Agric. Food Chem. 54 (2006) 4397–4406.
[9] Q.F. Zeng, Determination of amino acids and trace elements in Zhejiang Finger Citron, J. Jiaying Univ. 28 (2010) 75–77.
[10] X. Deng, X.M. Huang, D. Wu, Study on antioxidant activity and process optimization of extraction of polyphenols from Chuan Bergamot, Guangzhou Chem. Ind. 42 (2014) 50–53.
[11] B. Peng, J.N. Yang, W.J. Huang, D. Peng, S.X. Bi, L.Y. Song, Y. Wen, J.H. Zhu, Y. Y. Chen, R.M. Yu, Structural characterization and immunoregulatory activity of a novel heteropolysaccharide from bergamot (*Citrus medica* L. var. *sarcodactylis*) by alkali extraction, Ind. Crop. Prod. 140 (2019) 11617.
[12] M. Shojaemehr, M. Alamholo, J. Soltani, Investigation of antibacterial and antioxidant activity of *Citrus medica* L extract on human pathogenic bacteria, Avicenna J. Clin. Microbiol. Infect. 7 (2020) 8–14.
[13] N. Chhikara, R. Kour, S. Jaglan, P. Gupta, Y. Gat, A. Panghal, *Citrus medica*: nutritional, phytochemical composition and health benefifits - a review, Food Funct. 9 (2018) 1978–1992.
[14] M.H. Hetta, T.S. El-Alfy, N.Z. Yassin, R.F. Abdel-Rahman, E.M. Kadry, Phytochemical and antihyperglycemic studies on *Citrus medica* L. leaves (Etrog) growing in Egypt, Int. J. Pharmacogn. Phytochem. Res. 5 (2013) 271–277.
[15] M.A. Al-Yahya, R.A. Mothana, M.S. Al-Said, K.E. El-Tahir, M. Al-Sohaibani, S. Rafatullah, *Citrus medica* "Otroj": attenuates oxidative stress and cardiac dysrhythmia in isoproterenol-induced cardiomyopathy in rats, Nutrients 5 (2013) 4269–4283.
[16] H.Y. Gao, Q. Tian, Antidepressant effect essential oils of *C. medica* L. var. *sarcodactylis* Swingle in rats, Chin. J. Exp. Trad. Med. Formula. 18 (2012) 231–234.
[17] P.C. Kuo, Y.R. Liao, H.Y. Hung, C.W. Chuang, T.L. Hwang, S.C. Huang, Y.J. Shiao, D.H. Kuo, T.S. Wu, Anti-inflammatory and neuroprotective constituents from the peels of *Citrus grandis*, Molecules 22 (2017) 967.
[18] Q.G. Ma, R.R. Wei, B. Zhou, Z.P. Sang, W.M. Liu, Z.L. Cao, Antiangiogenic phenylpropanoid glycosides from *Gynura cusimbua*, Nat. Prod. Res. 33 (2019) 457–463.
[19] Q.G. Ma, R.R. Wei, D.L. Shang, Z.P. Sang, W.M. Liu, Z.L. Cao, Hepatoprotective and neuroprotective flavanes from the fruits of *Ulmus pumila* L. (Ulmaceae), Pak. J. Pharm. Sci. 32 (2019) 2059–2064.
[20] Q.G. Ma, R.R. Wei, Z.P. Sang, Structural characterization and hepatoprotective activity of naphthoquinone from *Cucumis bisexualis*, Nat. Prod. Commun. 15 (2020) 1–6.
[21] R.R. Wei, Q.G. Ma, G.Y. Zhong, J.W. He, Z.P. Sang, Isolation and characterization of flavonoid derivatives with anti-prostate cancer and hepatoprotective activities from the flowers of *Hosta plantaginea* (Lam.) Aschers, J. Ethnopharmacol. 253 (2020), 112685.
[22] Q.G. Ma, R.R. Wei, D.L. Shang, Z.P. Sang, J.H. Dong, Structurally diverse flavonolignans with immunosuppressive and neuroprotective activities from the fruits of *Hippophae rhamnoides* L, J. Agric. Food Chem. 68 (2020) 6564–6575.
[23] L. Zhen, J.Y. Zhao, S.F. Sun, Y. Li, J. Qu, H.T. Liu, Y.B. Liu, Sesquiterpenes from an endophytic *Aspergillus flavus*, J. Nat. Prod. 82 (2019) 1063–1071.
[24] Q.G. Ma, R.R. Wei, X.D. Zhang, Z.P. Sang, J.H. Dong, Q.X. Lu, H.F. Huang, D. M. Guo, L. Jiang, Tropolone derivatives with hepatoprotective and

antiproliferative activities from the aerial parts of *Chenopodium album* Linn, Fitoterapia 146 (2020), 104733.
[25] X.R. Peng, J.Q. Liu, C.F. Wang, X.Y. Li, Y. Shu, L. Zhou, M.H. Qiu, Hepatoprotective effects of triterpenoids from *Ganoderma cochlear*, J. Nat. Prod. 77 (2014) 737–743.
[26] L. Yang, Z.M. Wang, Y. Wang, R.S. Li, F. Wang, K. Wang, Phenolic constituents with neuroprotective activities from *Hypericum wightianum*, Phytochemistry 65 (2019), 112049.
[27] B.P. Jiang, Y.M. Liu, L. Le, Z.Y. Li, J.Y. Si, X.M. Liu, Q. Chang, R.L. Pan, Cajaninstilbene acid prevents corticosterone-induced apoptosis in PC12 cells by inhibiting the mitochondrial apoptotic pathway, Cell. Physiol. Biochem. 34 (2014) 1015–1026.
[28] D. Zhou, Y. Li, G. Chen, Y.Q. Yang, Y. Mi, B. Lin, W. Li, Y. Hou, N. Li, Structural elucidation and anti-neuroinflammatory activities of lignans from the testas of *Vernicia montana*, Bioorg. Chem. 97 (2020), 103690.
[29] F.H. Li, Z.Y. Cao, H.Q. Wang, C.K. Li, J. Fu, J. Xie, B.M. Li, R.Y. Chen, J. Kang, Inhibition of IL-6 expression by lignans and other constituents isolated from Schefflera rubriflora C. J. Tseng & G. Hoo, Fitoterapia 140 (2020) 104417.
[30] H.M. Wang, Z.T. Song, H.H. Xing, Z.Y. Shi, P. Wu, J. Zhang, M. Tuerhong, J. Xu, Y. Q. Guo, Nitric oxide *inh*ibitory iridoids as potential anti-inflammatory agents from *Valeriana jatamansi*, Bioorg. Chem. 101 (2020), 103974.
[31] C.M. Xiao, X.H. Jia, H.F. Du, H.X. Zhao, C.L. Du, W.Z. Tang, X.J. Wang, Three new *C*-geranylated flavonoids from *Paulownia catalpifolia* T. Gong ex D.Y. Hong seeds with their inhibitory effects on xanthine oxidase, Phytochem. Lett. 36 (2020) 162–165.
[32] Q.G. Ma, R.R. Wei, Z.P. Sang, J.H. Dong, Structural characterization, neuroprotective and hepatoprotective activities of flavonoids from the bulbs of *Heleocharis dulcis*, Bioorg. Chem. 96 (2020), 103630.
[33] Y. Zhu, R.Z. Huang, C.G. Wang, X.L. Ouyang, X.T. Jing, D. Liang, H.S. Wang, New inhibitors of matrix metalloproteinases 9 (MMP-9): Lignans from *Selaginella moellendorffii*, Fitoterapia 130 (2018) 281–289.
[34] L. Cheng, D.L. Guo, M.S. Zhang, L.H. Lang, S.B. Fu, Y. Deng, Y.Q. He, S.J. Xiao, Dihydrophenanthrofurans and bisbibenzyl derivatives from the stems of *Dendrobium nobile*, Fitoterapia 143 (2020), 104586.
[35] Z.J. Ye, X.A. He, J.P. Wu, J. Li, X.W. Chang, J. Tan, W.Y. Lv, H. Zhu, H.H. Sun, W. X. Wang, Z.H. Chen, G.Z. Zhu, K.P. Xu, New prenylflavonol glycosides with xanthine oxidase inhibitory activity from the leaves of *Cyclocarya paliurus*, Bioorg. Chem. 101 (2020), 104018.
[36] T. Tanaka, T. Nakashima, T. Ueda, K. Tomii, I. Kouno, Facile discrimination of aldose enantiomers by reversed-phase HPLC, Chem. Pharm. Bull. 55 (2007) 899–901.
[37] L. Gonzalez-Cofrade, S. Oramas-Royo, I. Cuadrado, A. Amesty, S. Hortelano, A. Estevez-Braun, B. Heras, Dehydrohispanolone derivatives attenuate the inflammatory response through the modulation of inflammasome activation, J. Nat. Prod. 83 (2020) 2155–2164.
[38] Y.P. Liu, X.M. Yu, W. Zhang, T. Wang, B. Jiang, H.X. Tang, Q.T. Su, Y.H. Fu, Prenylated chromones and flavonoids from *Artocarpus heterophyllus* with their potential antiproliferative and anti-inflammatory activities, Bioorg. Chem. 101 (2020), 104030.
[39] D.D. Huang, X. Wang, L. Sun, W.S. Chen, L.N. Sun, Two new phenylpropanoids from *Penthorum chinens*e Pursh, Phytochem. Lett. 28 (2018) 84–87.
[40] Q.G. Ma, R.R. Wei, M. Yang, X.Y. Huang, F. Wang, Z.P. Sang, W.M. Liu, Q. Yu, Molecular characterization and bioactivity of coumarin derivatives from the fruits of *Cucumis bisexualis*, J. Agric. Food Chem. 66 (2018) 5540–5548.
[41] S.J. Zhang, Y.Y. Huang, Y. Li, Y.H. Wang, X.J. He, Anti-neuroinflammatory and antioxidant phenylpropanoids from Chinese olive, Food Chem. 286 (2019) 421–427.
[42] Y.X. Ma, H. Wang, R. Wang, F.C. Meng, Z.Y. Dong, G.W. Wang, X.Z. Lan, H. Quan, Z.H. Liao, M. Chen, Cytotoxic lignans from the stems of *Herpetospermum pedunculosum*, Phytochemistry 164 (2019) 102–110.
[43] L. Xiao, Y.Y. Huang, Y.H. Wang, J.W. Xu, X.G. He, Anti-neuroinflammatory benzofurans and lignans from *Praxelis clematidea*, Fitoterapia 140 (2020), 104440.
[44] Q.G. Ma, Y.G. Wang, W.M. Liu, R.R. Wei, J.B. Yang, A.G. Wang, T.F. Ji, J. Tian, Y. L. Su, Hepatoprotective sesquiterpenes and rutinosides from *Murraya koenigii* (L.) Spreng, J. Agric. Food Chem. 62 (2014) 4145–4151.
[45] Q.G. Ma, R.R. Wei, M. Yang, X.Y. Huang, G.Y. Zhong, Z.P. Sang, J.H. Dong, J. C. Shu, J.Q. Liu, R. Zhang, J.B. Yang, A.G. Wang, T.F. Ji, Y.L. Su, Structures and biological evaluation of phenylpropanoid derivatives from *Murraya koenigii*, Bioorg. Chem. 86 (2019) 159–165.